



UNIVERSITY OF LEEDS

This is a repository copy of *Versailles Project on Advanced Materials and Standards interlaboratory study on intensity calibration for x-ray photoelectron spectroscopy instruments using low-density polyethylene*.

White Rose Research Online URL for this paper:  
<http://eprints.whiterose.ac.uk/168698/>

Version: Accepted Version

---

**Article:**

Reed, BP, Cant, DJH, Spencer, SJ et al. (48 more authors) (2020) Versailles Project on Advanced Materials and Standards interlaboratory study on intensity calibration for x-ray photoelectron spectroscopy instruments using low-density polyethylene. *Journal of Vacuum Science & Technology A*, 38 (6). 063208. 063208-1-063208-15. ISSN 0734-2101

<https://doi.org/10.1116/6.0000577>

---

© 2020 Author(s). This article may be downloaded for personal use only. Any other use requires prior permission of the author and AIP Publishing. The following article appeared in Reed, BP, Cant, DJH, Spencer, SJ et al. (48 more authors) (2020) Versailles Project on Advanced Materials and Standards interlaboratory study on intensity calibration for x-ray photoelectron spectroscopy instruments using low-density polyethylene. *Journal of Vacuum Science & Technology A*, 38 (6). 063208. 063208-1-063208-15 and may be found at <https://avs.scitation.org/doi/full/10.1116/6.0000577>. Uploaded in accordance with the publisher's self-archiving policy.

**Reuse**

Items deposited in White Rose Research Online are protected by copyright, with all rights reserved unless indicated otherwise. They may be downloaded and/or printed for private study, or other acts as permitted by national copyright laws. The publisher or other rights holders may allow further reproduction and re-use of the full text version. This is indicated by the licence information on the White Rose Research Online record for the item.

**Takedown**

If you consider content in White Rose Research Online to be in breach of UK law, please notify us by emailing [eprints@whiterose.ac.uk](mailto:eprints@whiterose.ac.uk) including the URL of the record and the reason for the withdrawal request.



[eprints@whiterose.ac.uk](mailto:eprints@whiterose.ac.uk)  
<https://eprints.whiterose.ac.uk/>

**Supporting Information for  
VAMAS Inter-laboratory study on intensity calibration for XPS instruments  
using low-density polyethylene**

Benjamin P. Reed\*<sup>1</sup>, David J. H. Cant<sup>1</sup>, Steve J. Spencer<sup>1</sup>, Abraham Jorge Carmona-Carmona<sup>2</sup>, Adam Bushell<sup>3</sup>, Alberto Herrera-Gómez<sup>2</sup>, Akira Kurokawa<sup>4</sup>, Andreas Thissen<sup>5</sup>, Andrew G. Thomas<sup>6</sup>, Andrew J. Britton<sup>7</sup>, Andrzej Bernasik<sup>8</sup>, Anne Fuchs<sup>9</sup>, Arthur P. Baddorf<sup>10</sup>, Bernd Bock<sup>11</sup>, Bill Theilacker<sup>12</sup>, Bin Cheng<sup>13</sup>, David G. Castner<sup>14</sup>, David J. Morgan<sup>15</sup>, David Valley<sup>16</sup>, Elizabeth A. Willneff<sup>17</sup>, Emily F. Smith<sup>18</sup>, Emmanuel Nolot<sup>19</sup>, Fangyan Xie<sup>20</sup>, Gilad Zorn<sup>21</sup>, Graham C. Smith<sup>22</sup>, Hideyuki Yasufuku<sup>23</sup>, Jeffery Fenton<sup>24</sup>, Jian Chen<sup>20</sup>, Jonathan D. P. Counsell<sup>25</sup>, Jörg Radnik<sup>26</sup>, Karen J. Gaskell<sup>27</sup>, Kateryna Artyushkova<sup>16</sup>, Li Yang<sup>28</sup>, Lulu Zhang<sup>4</sup>, Makiho Eguchi<sup>29</sup>, Marc Walker<sup>30</sup>, Mariusz Hajdyla<sup>8</sup>, Mateusz M. Marzec<sup>8</sup>, Matthew R. Linford<sup>31</sup>, Naoyoshi Kubota<sup>29</sup>, Orlando Cortazar-Martínez<sup>2</sup>, Paul Dietrich<sup>5</sup>, Riki Satoh<sup>29</sup>, Sven L. M. Schroeder<sup>7</sup>, Tahereh G. Avval<sup>31</sup>, Takaharu Nagatomi<sup>32</sup>, Vincent Fernandez<sup>33</sup>, Wayne Lake<sup>34</sup>, Yasushi Azuma<sup>4</sup>, Yusuke Yoshikawa<sup>35,36</sup>, and Alexander G. Shard<sup>1</sup>

\*Corresponding author: Tel: +44 (0)20 8943 6952; E-mail: [benjamin.reed@npl.co.uk](mailto:benjamin.reed@npl.co.uk)

<sup>1</sup> National Physical Laboratory, Hampton Road, Teddington, TW11 0LW, UK.

<sup>2</sup> CINVESTAV-Unidad Queretaro, Queretaro 76230, Mexico.

<sup>3</sup> Thermo Fisher Scientific (Surface Analysis), East Grinstead, RH19 1XZ, UK.

<sup>4</sup> National Metrology Institute of Japan (NMIJ), National Institute of Advanced Industrial Science and Technology (AIST), 1-1-1 Higashi, Tsukuba, Ibaraki 305-8565, Japan.

<sup>5</sup> SPECS Surface Nano Analysis GmbH, Voltastraße 5, 13355 Berlin, Germany.

<sup>6</sup> Department of Materials, Photon Science Institute and Sir Henry Royce Institute, Alan Turing Building, University of Manchester, Oxford Road, Manchester, M13 9PL, UK.

<sup>7</sup> Versatile X-ray Spectroscopy Facility, School of Chemical and Process Engineering, University of Leeds, Leeds, LS2 9JT, UK.

<sup>8</sup> Academic Centre for Materials and Nanotechnology, AGH University of Science and Technology, 30-059 Kraków, Poland.

<sup>9</sup> Robert Bosch GmbH, Robert-Bosch-Campus, 71272 Renningen, Germany.

<sup>10</sup> Center for Nanophase Materials Sciences, Oak Ridge National Laboratory, 1 Bethel Valley Rd, Oak Ridge, TN 37830, USA.

<sup>11</sup> Tascon GmbH, Mendelstr. 17, D-48149 Münster, Germany.

<sup>12</sup> Medtronic, 710 Medtronic Parkway, LT240, Fridley, MN 55432, USA.

<sup>13</sup> Analysis and Testing Center, Beijing University of Chemical Technology, Beijing 100029, P. R. China.

<sup>14</sup> National ESCA and Surface Analysis Center for Biomedical Problems, Department of Bioengineering and Chemical Engineering, University of Washington, Seattle, Washington 98195, USA.

<sup>15</sup> Cardiff Catalysis Institute, School of Chemistry, Cardiff University, Main Building, Cardiff CF10 3AT, UK.

- <sup>16</sup> Physical Electronics Inc., East Chanhassen, Minnesota 55317, USA.
- <sup>17</sup> Versatile X-ray Spectroscopy Facility, School of Design, University of Leeds, Leeds, LS2 9JT, UK.
- <sup>18</sup> Nanoscale and Microscale Research Centre, University of Nottingham, Nottingham, NG7 2QB, UK.
- <sup>19</sup> CEA-LETI, 17 rue des Martyrs, 38054 Grenoble, France.
- <sup>20</sup> Instrumental Analysis & Research Center, Sun Yat-sen University, Guangzhou 510275, P. R. China.
- <sup>21</sup> GE Research, 1 Research Circle, K1 1D7A, Niskayuna, NY 12309, USA.
- <sup>22</sup> Faculty of Science and Engineering, University of Chester, Thornton Science Park, Chester, CH2 4NU, UK.
- <sup>23</sup> Materials Analysis Station, National Institute for Materials Science (NIMS), 1-2-1 Sengen, Tsukuba, Ibaraki 305-0044, Japan.
- <sup>24</sup> Medtronic, 6700 Shingle Creek Parkway, Brooklyn Center, MN 55430, USA.
- <sup>25</sup> Kratos Analytical Ltd., Wharfside, Trafford Wharf Road, Manchester M17 1GP, UK.
- <sup>26</sup> Bundesanstalt für Materialforschung und -prüfung (BAM), Unter den Eichen 44-46, 12203 Berlin, Germany.
- <sup>27</sup> Department of Chemistry and Biochemistry, University of Maryland, College Park, MD 20742, USA.
- <sup>28</sup> Department of Chemistry, Xi'an Jiaotong-Liverpool University, Suzhou Dushu Lake Higher Education Town, P. R. China.
- <sup>29</sup> Surface Analysis Dep. Materials Characterization Div., Futtsu Unit. NIPPON STEEL TECHNOLOGY Co.,Ltd., Japan.
- <sup>30</sup> Department of Physics, University of Warwick, Coventry, West Midlands, CV4 7AL, UK.
- <sup>31</sup> Department of Chemistry and Biochemistry, Brigham Young University, Provo, UT 84604, USA.
- <sup>32</sup> Platform Laboratory for Science and Technology, Asahi Kasei Corporation, 2-1 Samejima, Fuji, Shizuoka 416-8501, Japan.
- <sup>33</sup> Institut des matériaux Jean Rouxel, 44300 Nantes, France.
- <sup>34</sup> Atomic Weapons Establishment (AWE), Aldermaston, Reading, Berkshire, RG7 4PR, UK.
- <sup>35</sup> Material Analysis Department, Yazaki Research and Technology Center, YAZAKI Corporation, Susono City, Japan.
- <sup>36</sup> Technical & Project Support Dept., Nidec Sankyo CMI Corporation, 46-1, Senpuku, Susono-city, Shizuoka 460-1116, Japan (current address).

## **S1: Inter-laboratory Study Protocol**

The following protocol was included in the sample package that was shipped to all participants of the VAMAS TWA 2, Project A27: “Intensity calibration for XPS instruments using low-density polyethylene”. A digital draft of the protocol was distributed to the participants in advance of the study so that they could suggest changes or ask for clarification. This protocol has been designated “NPL Report AS 100”.

*N.B. This VAMAS inter-laboratory study has concluded and the organisers stated herein are no longer accepting data or results. An up-to-date improved LDPE calibration protocol has been detailed in the main manuscript.*

### ***Abstract***

This report outlines the analysis protocol for an interlaboratory study conducted under the auspices of VAMAS TWA 2 (Surface Chemical Analysis) for the intensity calibration for XPS instruments using polyethylene. The protocol involves the use of low-density polyethylene, prepared using a clean scalpel to remove surface oxygen, as a secondary calibration standard. For monochromated Al K $\alpha$  sources, the acquired spectrum is used in conjunction with a mathematically generated polyethylene reference spectrum to determine a representative transmission function. A rational function is then fitted to produce a noise-free continuous transmission function description which can be used to intensity-correct spectra from other materials. Participants will also acquire a spectrum from sputter-cleaned gold for validation purposes. This report will guide VAMAS participants through the sample preparation, calibration process, and reporting of their results. For non-monochromated sources, the study will enable an assessment of whether polyethylene could also be used as a secondary calibration standard.

### ***1 Introduction***

X-ray photoelectron spectroscopy (XPS) is a highly surface sensitive, ultra-high vacuum technique capable of quantitatively measuring the elemental composition and the chemical state of a material’s surface. Accurate and precise analysis of photoelectron spectra relies on a well-calibrated spectrometer, both in the kinetic energy scale and the intensity scale. For this study, only the intensity calibration is considered. Photoelectron analysers rely on electrostatic and magnetic lens systems to guide electrons into the deflection hemispheres via the entrance plane and retard their velocities to match the chosen pass energy. The efficiency at which the lens system samples photoelectrons at different kinetic energies is known as the analyser’s transmission function  $T(E)$ , and this function changes for different acquisition modes, pass energies, X-ray spot sizes, and aperture settings. To obtain accurate intensities, and hence elemental compositions, from an XPS spectrum without the use of reference materials, the data must be  $T(E)$  corrected.

The purpose of this inter-laboratory study is to assess the validity of a new intensity calibration method for determining a spectrometer’s  $T(E)$  using low-density polyethylene (LDPE) as a cheap and easy-to-prepare alternative to gold, silver, and copper calibration standards. In

contrast to these calibration standards, LDPE does not require ion sputtering to decontaminate the surface and is insensitive to hydrocarbon contamination; a clean oxygen-free surface can be obtained by scraping the surface of the LDPE with a clean metal scalpel. A LDPE spectrum contains far fewer photoelectron and Auger peaks than other metal calibration standards making it simple enough to be described by a mathematical function. This means that a nearly continuous noise-free reference spectrum can be obtained. The potential issue arises from the need for longer acquisition times and therefore the necessity for dark noise removal due to LDPEs low photoelectron yield.

The T(E) calculated from this protocol will be used to correct a sputter-cleaned gold spectrum from the same spectrometer, and this corrected spectrum will be compared against spectra from other laboratories and traceable reference spectra of gold, taking into account the instrument's geometry. The variance between these T(E) corrected spectra will be assessed to determine whether the LDPE secondary standard intensity calibration qualifies as a suitable T(E) correction method.

## **2      *Contacts & Timetable***

This VAMAS interlaboratory study is being coordinated by the National Physical Laboratory, UK under the auspices of VAMAS TWA 2 (Surface Chemical Analysis). Your contacts for this study are Benjamen Reed (benjamen.reed@npl.co.uk) and Alexander Shard (alex.shard@npl.co.uk). If any part of this protocol is unclear or you obtain unexpected results, please contact us immediately.

You should complete the analysis for this work by 1st August 2019. If you are unable to do so and require extra time, please inform Benjamen Reed or Alexander Shard.

## **3      *This Package***

This package contains this protocol, a LDPE sample, a gold foil, and a clean scalpel. The LDPE and gold are contained in 1" polypropylene wafer trays. Upon receipt of this package, please inform NPL that you have received it and that all items are accounted for. There is also a 'notice to customs' which should inform you if the samples have been handled by customs / postal staff.

I have e-mailed NPL to confirm that all is okay with the sample(s) on:  
/ / 2019

## **4      *Samples***

Low-density polyethylene (LDPE) is a thermoplastic with general formula  $(C_2H_4)_n$ . LDPE is used in applications mostly pertaining to containers, packaging, and tubing due to its excellent chemical resistance, flexibility, and toughness. Importantly, it is easy to handle and not toxic or harmful. In this XPS study, LDPEs simple chemical structure results in a spectrum with few peaks and an easily described inelastic background.

LDPE samples should be stored in a dark, clean, and dust-free environment. LDPE can be stored for years without degradation, although long-term oxidation does occur on the surface. A standard solvent rinse (i.e. acetone, isopropanol, methanol / deionized water rinse) is not recommended because, despite LDPEs compatibility with these solvents, they may leave residues on the surface or cause the LDPE to swell. The samples should be analysed as soon as convenient and before the deadline stated in Section 2.

To prepare the sample for analysis, mount the LDPE onto the spectrometer sample stage or stub. If required, the sample can be cut down to a smaller size using a clean pair of scissors. A fresh surface of LDPE is prepared using a clean flat-bladed metal scalpel; firmly scrape the surface of the LDPE several times until the surface turns from shiny to matte. Also ensure that the direction of last few scrapes are parallel to the monochromator-sample-analyser plane to reduce the X-ray shadowing effect of any directional topography induced by the cleaning process. Always make sure to scrape away from yourself to avoid injury.

Immediately place the sample into the XPS load lock and begin pumping down. Move the sample into the UHV analysis chamber as soon as possible. If sample preparation is performed correctly, the O 1s signal in XPS should be below the detection limit which is less than 0.03 at%.

A gold sample should also be prepared for XPS analysis using whatever methods your lab has to ensure a clean contaminant-free surface, preferably ion sputtering in-vacuo. The analysis should be performed in a manner that prevents cross-contamination between the gold and LDPE samples. For example, avoid sputtering the gold before completing the LDPE analysis.

## **5 Instrument Operating Conditions**

### **5.1 XPS Analysis of Polyethylene**

The complete intensity calibration procedure is suitable for spectrometers which use a monochromatic Al K $\alpha$  X-ray source. The anode, monochromator, sample, and analyser entrance should be in the same plane and the angle between the incident X-rays and the emitted photoelectrons should be close to the magic angle (i.e. 54.7°). For other instruments, the complete calibration procedure may not be applicable, and it is part of the interlaboratory study to identify the range of applicability and whether modifications to the procedure will extend that range. If your instrument does not meet these criteria, please proceed as described below, but note that there may be issues and discrepancies in the data processing. Provided that the data are collected and reported as described in the document, they are still useful and will be analysed at NPL.

The selected area of analysis for XPS on the LDPE should be free of contaminants, most notably oxygen. A LDPE sample prepared according to Section 4 will not have any surface oxygen or foreign contaminants present across the entire PE surface. **Figure S2 in Section 6.1.1** shows an example of survey scans for a properly prepared LDPE surface and an unacceptable surface respectively. If the selected analysis area shows no evidence of an O 1s, O KLL peak, or other contaminating elements, then it is appropriate to continue with XPS analysis.

## 5.2 XPS Analysis of Gold

A survey spectrum of contaminant-free gold should also be acquired. The transmission function of a spectrometer can change over time, so it is important that this gold spectrum is acquired around the same time as the LDPE spectra, preferably on the same day.

The data should be reported as raw intensities in counts per second without transmission function correction. The energy scale should be in kinetic energy. Feel free to apply this procedure to as many lens modes and pass energies as you wish, but we do ask, as a minimum, that you provide data for a high pass energy (i.e. typical survey scan pass energy) with a fully open entrance slit/aperture.

## 5.3 Charge Compensation

LDPE is an insulator and therefore sample charging is expected. To ensure the correct background shape, charge neutralisation must be used. **Figure S1** shows the C 1s peak before and after charge compensation using an electron flood gun has been applied.

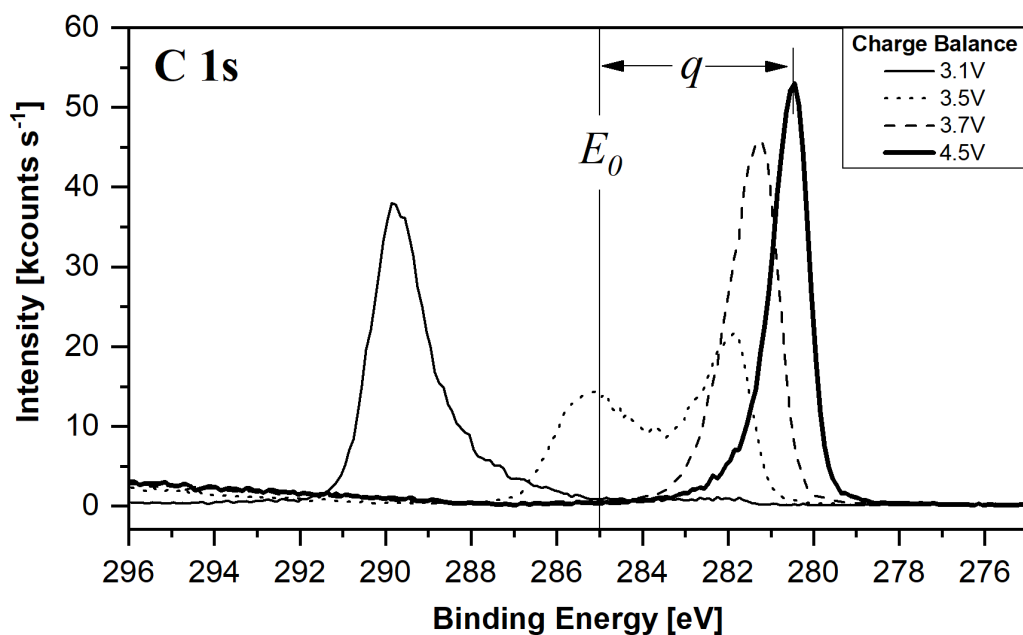


**Figure S1.** C 1s peak measured from a polyethylene sample for different charge compensation parameters. The bold line shows the correct line shape for the C 1s peak. The peak may be offset by  $q$  from  $E_0$ , which is the charge reference energy of C 1s that minimises the residual between the mathematically generated LDPE spectrum and the acquired LDPE spectrum (see Section 6.3.1.).

## 6 *Data Acquisition and Analysis*

In general, the objectives of this study are:

1. Acquire oxygen-free LDPE survey spectra and combine into a single low-noise spectrum.
2. Acquire a contaminant-free gold spectrum.
3. Divide the acquired LDPE spectrum by the reference LDPE spectrum to obtain a representation of the spectrometer's transmission function,  $Q(E)$ .
4. Extrapolate  $Q(E)$  to higher kinetic energies for fitting.
5. Fit a rational function to  $Q(E)$  to obtain a continuous, noise-free  $T(E)$ .

### 6.1 *Acquisition*

#### 6.1.1 *LDPE Spectra*

Without turning the X-rays on, acquire a survey spectrum from 180 eV to 1500 eV (1280 eV for Mg  $K\alpha$  sources) kinetic energy. With the sample well out of the way of the analysis position, switch on the X-ray source and allow at least half an hour for the instrument to equilibrate. During this time, run several spectra in the high kinetic energy region above the X-ray source energy to determine the spectrometer's dark noise count rate. Make sure that the sample and sample holder is not in the X-ray beam during the dark noise acquisition, especially if you are operating a non-monochromated X-ray source. Now move the sample into the analysis position and optimise the sample height and charge compensation settings (see Section 5.2). The C 1s peak should be a single peak with the maximum count rate between 1200 eV and 1206 eV kinetic energy (967 eV to 973 eV for Mg  $K\alpha$  sources).

Once a suitable analysis area has been chosen, acquire a survey scan from 180 eV to 1500 eV kinetic energy using a high pass energy. Make sure that no elements other than carbon are detectable. If you observe any contaminating species and are unable to find an analysis region devoid of contaminants, remove the sample from the system, repeat the sample preparation outlined in Section 5 and start again. **Figure S2** provides example XPS survey scans that illustrate an acceptable and an unacceptable sample surface condition. Change the spectrometer settings to the lens mode and pass energy that requires calibration and allow at least five minutes for the instrument to equilibrate.

Acquire an initial survey spectrum from 180 eV to 1500 eV (1280 eV for Mg  $K\alpha$  sources) kinetic energy. The low count rate region between the C 1s peak and the valence band will require acquisition times 30 to 40 times greater than the rest of the spectrum, so also acquire at least 30 spectra between 1195 eV and 1500 eV (960 eV to 1280 eV for Mg  $K\alpha$  sources) using the same step size and dwell time as the initial survey. If possible, ensure that the start energy in the scan has the same kinetic energy as one of the data points in the initial survey spectrum. Acquire a final survey spectrum from 180 eV to 1500 eV (1280 eV for Mg  $K\alpha$  sources) kinetic energy. It is recommended that a step size of approximately 1 eV is used.

At the end of the LDPE acquisition stage, the following datasets should be saved:

1. Survey spectrum with X-ray source OFF
2. High Kinetic Energy Spectra with X-ray source ON



3. Initial Survey
4. High KE Region (multiple acquisitions)
5. Final Survey

This acquisition procedure should be repeated on a fresh area of the sample for every operating mode of the instrument that needs to be calibrated. There should be the five datasets listed above for every lens mode and pass energy that needs to be calibrated. The data should be exported without transmission function correction and the intensity should be stated in counts per second.

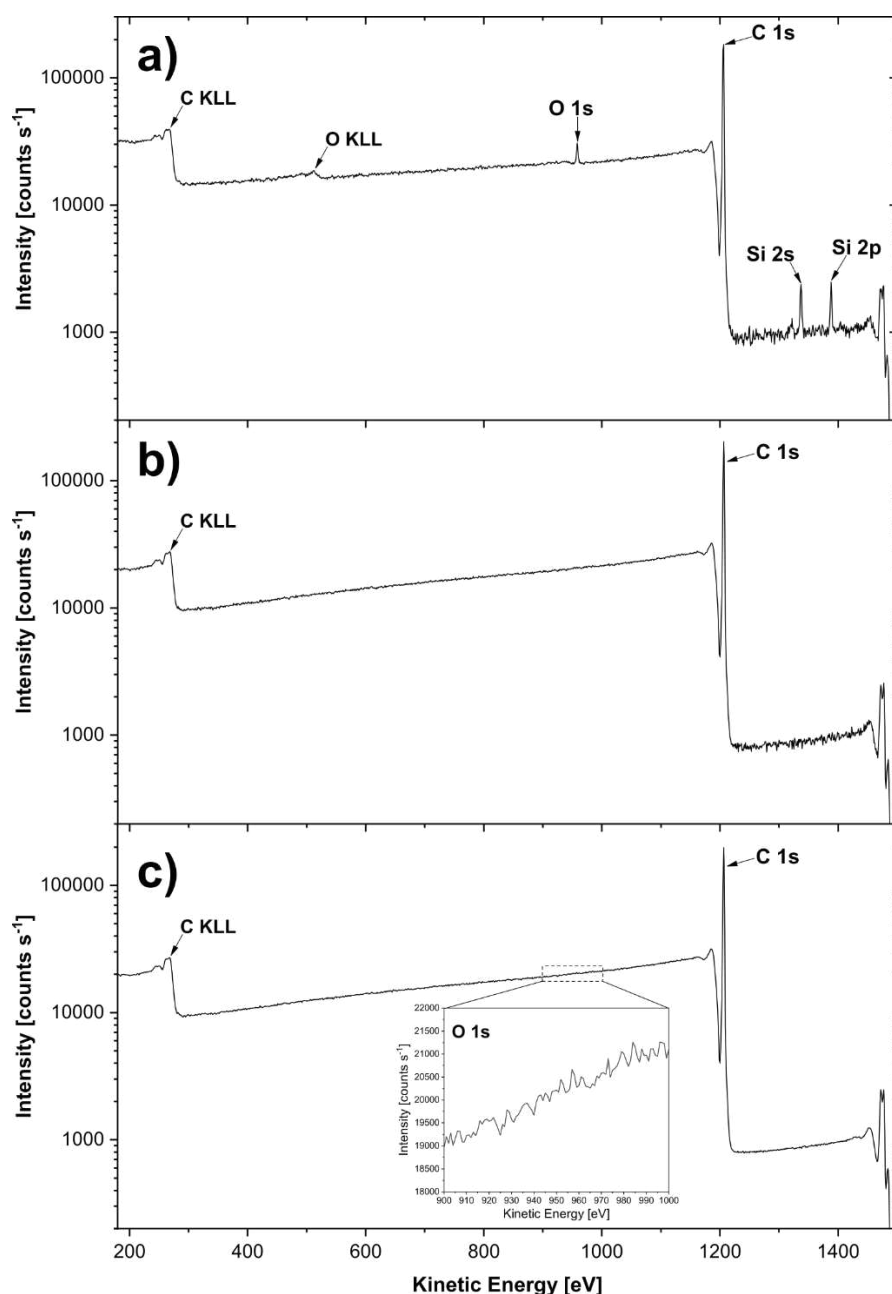


**Figure S2.** A comparison between (a) a bad survey scan, (b) a good survey scan, and (c) the average combined spectra (see Section 6.2). The acceptable scans (b, c) show no evidence of contamination whereas the bad scan (a) has oxygen and silicon contaminants which impart a significant change in the background, especially in the low kinetic region near the C KLL feature.

### 6.1.2 Gold Spectrum

For each lens mode and pass energy that LDPE spectra were acquired, a corresponding gold spectrum should also be obtained. Load the gold sample into the spectrometer and use ion sputtering to remove all surface contaminants. Move the sample into the analysis position and optimise the sample height to obtain the maximum count rate in the Au 4f peak (~84 eV binding energy). Acquire a spectrum over a kinetic energy range between 180 eV and 1500 eV. The data should be exported without transmission function correction and the intensity should be stated in counts per second.

### 6.2 Combining LDPE Spectra

Organic materials are known to degrade under X-ray illumination, which possibly affects the intensity of the inelastic background. In the case of LDPE, little-to-no change is expected because even if chemical damage occurs, the loss of hydrogen should not strongly affect the spectrum. Nevertheless, the effects of sample damage and spectrometer performance with time, for each lens mode and pass energy, should be tested.

For each lens mode / pass energy, take the final survey scan and divide it by the initial survey scan. Plot this intensity ratio (final : initial) against kinetic energy to produce a plot similar to **Figure S3**. From this plot, any changes in the acquisition conditions can be diagnosed. In **Figure S3**, there is a systemic reduction in intensity between 2% and 3%. **Figure S3** also illustrates that the region with kinetic energies higher than the C 1s peak has a much larger noise, justifying the longer acquisitions times demanded in Section 6.1 for this region of the spectrum.

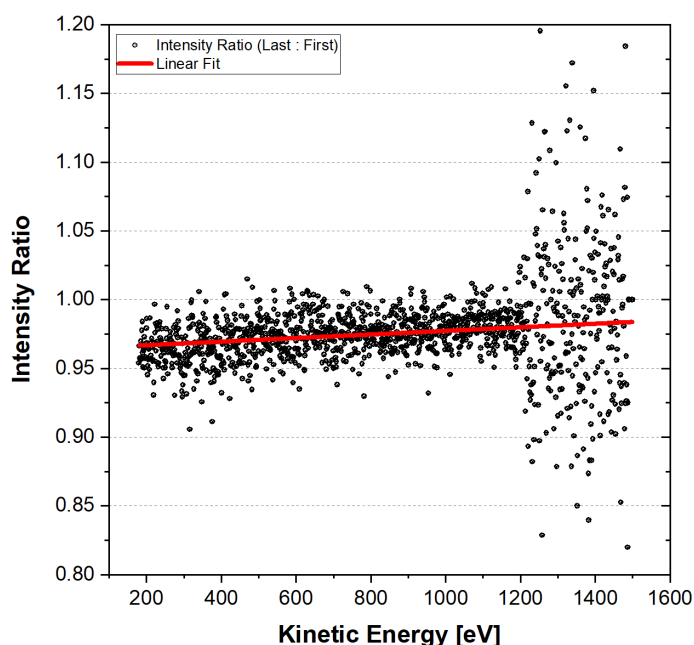


**Figure S3.** XPS Survey of fresh LDPE divided by survey taken after 3 hours of X-ray exposure. The systematic shift of 0.02 - 0.03 is attributed to changes in the MCP condition over time. Your Final:Initial ratio should be flat, but systematic shifts from unity are acceptable as long as they are not greater than 5%.

Combine the spectra numbers 3 to 5 (excluding the dark noise spectrum) into a single spectrum in counts per second against kinetic energy for each lens mode / aperture size / pass energy. To do this, take the average of all the spectra at each kinetic energy remembering that there are only two spectra to combine at low kinetic energy, but more than 30 at high kinetic energy. Determine the average dark noise as the average value of spectrum 1 in counts per second. Now subtract the average dark noise counts per second across the combined spectrum to obtain  $I$ , the dark noise corrected average spectrum of polyethylene.

If the spectrum is generated using monochromatic Al  $K\alpha$  X-rays, proceed to Section 6.3. Otherwise proceed to Section 7 and 8.

### 6.3 Analysis: Determining the Transmission Function

#### 6.3.1 Generating the LDPE Reference Spectra

To generate the LDPE reference spectrum, a mathematical description containing six components is used. Three of these components account for the steps in the inelastic background at the valence band, the C 1s peak, and the C  $KLL$  peak. The other three components are Gaussian peaks, two of which describe the C  $KLL$  features and the third describes long-range variations in intensity apparent in the background between the C 1s and C  $KLL$  peaks. Equation (SE1) is the summation of these six components which form the reference LDPE spectrum,  $I_{ref}$ .

$$I_{ref} = \sum_{i=1}^3 \left( \left\{ b_i \left[ \exp\left(\frac{\varepsilon}{c_i}\right) + d_i \right] \left[ 1 - \Phi\left(\frac{\varepsilon - e_i}{5}\right) \right] \right\} + \left\{ f_i \phi\left(\frac{\varepsilon - g_i}{h_i}\right) \right\} \right) \quad (SE1)$$

The constants of equation (SE1) are  $b_i$  to  $h_i$  and are required to reproduce the LDPE reference spectrum for a typical instrument geometry. These constants have been determined by fitting equation (SE1) to a LDPE reference spectrum calibrated to the NPL metrology spectrometer and are listed in table 1. DO NOT use equation (SE1) to fit your data, as this will not be  $I_{ref}$ . In equation (SE1), the capital phi  $\Phi$  is a cumulative normal distribution with mean  $e_i$  and a standard deviation of 5 eV. The lower-case phi  $\phi$  is a normal distribution (normalised Gaussian) with a mean  $g_i$  and a standard deviation  $h_i$ . The independent variable in equation (SE1) represents the charge corrected kinetic energies of the electrons,  $\varepsilon$ , which is calculated by:

$$\varepsilon = E + q \quad (SE2)$$

where  $E$  is the electron kinetic energy, and  $q$  is a variable static charge correction. For now, set  $q = 0$  but later it will be adjusted to correct for charge compensation and reduce the residual between  $I$  and  $I_{ref}$ .

**Table S1.** Parameters to recreate  $I_{ref}$  using equation (SE1)

$i$	1	2	3
<b>Values for step functions</b>			
<b>Feature</b>	C $KLL$	C 1s	Valence
<b>Intensity, <math>b_i</math> [<math>I_x</math>]</b>	2.04	0.638	0.0204
<b>Decay energy, <math>c_i</math> [eV]</b>	276	423	450

Constant, $d_i$	0	3.37	0
Position, $e_i$ [eV]	264	1201	1485
<b>Values for the normal distributions representing peaks</b>			
Peak	C <i>KLL</i> (minor)	C <i>KLL</i> (major)	Broad peak
Area, $f_i$ [ $I_x \cdot \text{eV}$ ]	6.36	50	612
Position, $g_i$ [eV]	242	264	685
Sigma width, $h_i$ [eV]	4.0	4.9	228

### 6.3.2 Calculating $Q(\varepsilon)$ and static charge correction

Once  $I$  and  $I_{ref}$  have been produced, use equation (SE3), to obtain the ratio  $Q(\varepsilon)$  which provides a visual representation of the spectrometer's *transmission function*.

$$Q(\varepsilon) = \frac{I}{I_{ref}} \quad (\text{SE3})$$

The C 1s peak and the peaks in the valence band have not been considered in  $I_{ref}$  and so these regions will need to be removed before continuing. For consistency, please remove the regions with kinetic energy between 1150 eV to 1220 eV and greater than 1420 eV. The region between 200 eV and 300 eV is the C *KLL* feature which in  $Q(E)$  deviates considerably. Up to this point  $\varepsilon = E$  because  $q$  is set to zero and therefore the energy shift caused by sample charging has not yet been corrected. By adjusting  $q$ , the sharp feature due to C *KLL* can be reduced to a minimum. From this point forward, the static charge corrected kinetic energy  $\varepsilon$  will be used for our calculations.

**Figure S4** gives an indication of what  $Q(\varepsilon)$  may look like after  $q$  has been set correctly and which regions to omit from the subsequent analysis.

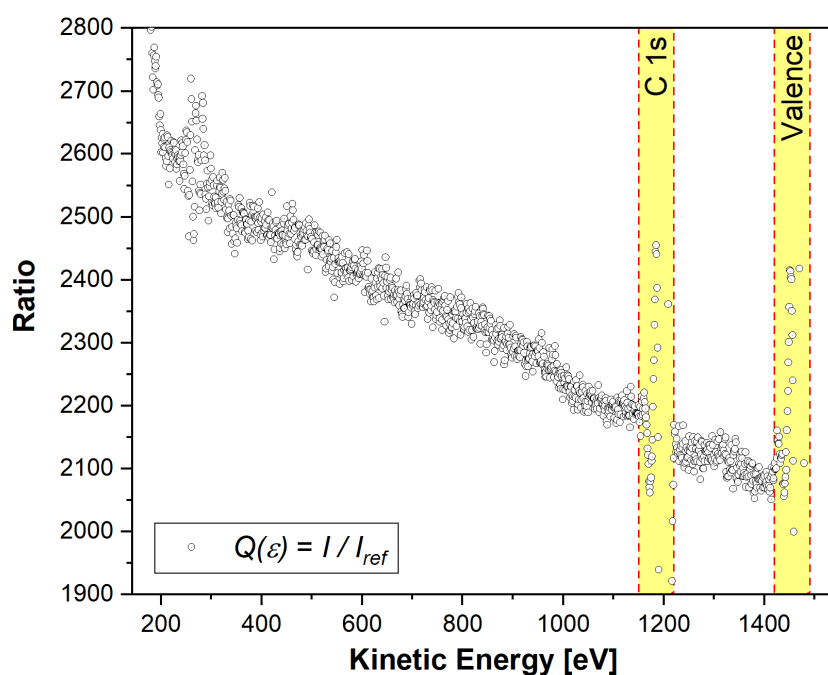


**Figure S4.** An example  $Q(\varepsilon)$  ratio plot with the regions to omit clearly marked.

### 6.3.3 Extrapolating $Q(\varepsilon)$ to Higher Kinetic Energies

If the fitting procedure in Section 7.3.4 is implemented on  $Q(\varepsilon)$  as calculated, then the fit beyond 1420 eV can diverge unrealistically from the true  $T(E)$ . Therefore, it is necessary to extrapolate the  $Q(\varepsilon)$  beyond this point to at least 2000 eV kinetic energy using a power law. To do this, the logarithm of  $Q(\varepsilon)$  is plotted against the logarithm of  $\varepsilon$  over the kinetic energy range 1220 eV to 1420 eV and linear regression provides  $a$  and  $n$  for equation SE4.

$$X(\varepsilon) = a\varepsilon^n \quad (\text{SE4})$$

**Figure S5** demonstrates a fit to the  $Q(\varepsilon)$  shown in **Figure S4**. Once a function describing the higher kinetic energy region has been calculated, extrapolate  $Q(\varepsilon)$  to 2000 eV by appending values of  $X$ . It is sufficient to use eleven points between 1500 eV and 2000 eV with 50 eV separation. These would be spaced on the red line. The combination of  $Q(\varepsilon)$  and the additional points calculated from equation (SE4) is  $R(\varepsilon)$ .

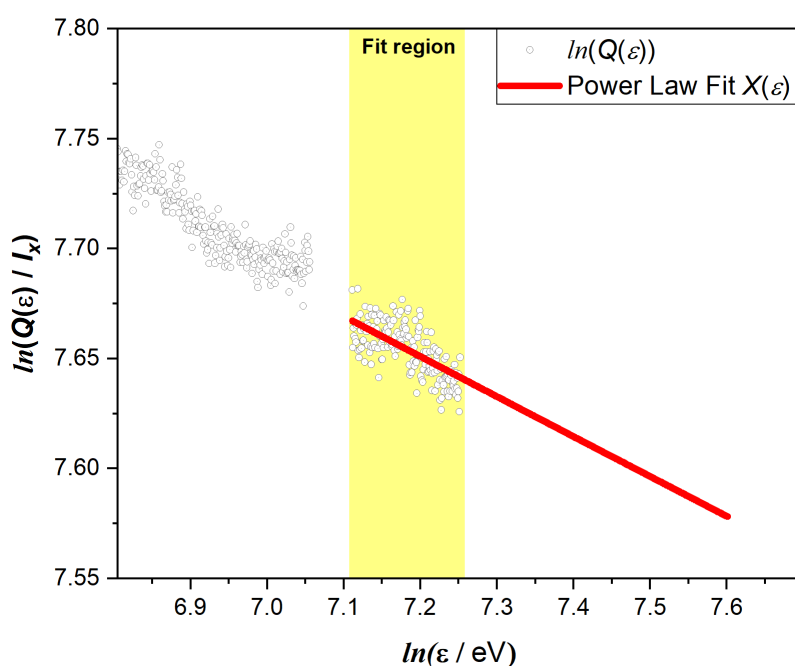


**Figure S5.** Extrapolation of  $\ln(Q(\varepsilon))$  using a power law fit from 1220 eV to 1420 eV and extended out to 2000 eV.

### 6.3.4 Fitting the Transmission Function $T(\varepsilon)$ to $R(\varepsilon)$

As mentioned in Section 6.3.2,  $Q(\varepsilon)$  is a representation of the spectrometer's transmission function. For future  $T(E)$  correction, a smooth description of  $Q(\varepsilon)$  is required over the range of kinetic energies where typical XPS experiments are conducted. A functional form which describes a wide range of instruments provided in equation (SE5),

$$T(E) = \frac{r_0 + \sum_{m=1}^k r_m \left( \frac{E}{1000} - 1 \right)^m}{1 + \sum_{n=1}^l s_n \left( \frac{E}{1000} - 1 \right)^n} \quad (\text{SE5})$$

where  $r_0$  is the value of  $T(1000 \text{ eV})$ , and  $r_m$  and  $s_n$  are coefficients of polynomial series of degree  $k$  and  $l$  respectively. Fit  $T(\varepsilon)$  to  $R(\varepsilon)$ . You may do this using any software, but you can also do it in the Excel spreadsheet sent to you as a participant in the study.

Using the Excel spreadsheet, ensure that the ‘Solver’ add-on in Excel is activated. The ‘Minimization Parameter’ is a root-sum-of-squares value derived from the residual of  $T(\varepsilon) - Q(\varepsilon)$  and should be the target of the ‘Set Objective Cell’ field. The objective should be set to ‘minimise’. The ‘By Changing Variable Cells’ should be set to change the values of  $r_0$ ,  $r_m$ , and  $s_n$  up to  $k = l = 4$ . The ‘Make Unconstrained Variable Non-Negative’ option should be unticked; the solving method should be set to ‘GRG Non-linear’. Click ‘Solve’ to initiate the fit. **Figure S6** shows what a successful fit may look like, with  $T(E)$  plotted between 200 eV and 1600 eV, a range which encapsulates the needs of most experiments. If the fit does not converge or deviates widely from  $Q(\varepsilon)$ , try the fitting procedure again but only include the terms for  $k = l = 1$  first, and then include higher-order terms in a second fitting attempt.

Once a suitable fit has been achieved, the  $T(\varepsilon)$  fitting parameters can be used to reproduce your spectrometer’s transmission function  $T(E)$  for any kinetic energy  $E$  for that pass energy and lens mode.

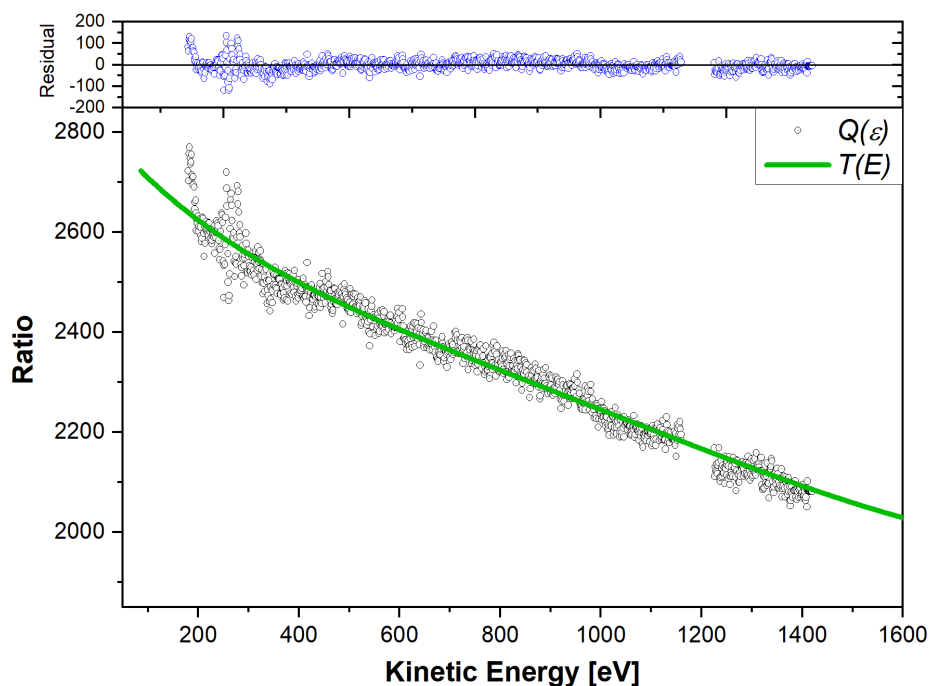


**Figure S6.** A correctly fitted transmission function  $T(E)$  to  $R(\varepsilon)$ . The extrapolation procedure ensures that the higher kinetic end of  $T(E)$  does not diverge significantly from the  $Q(\varepsilon)$  data. This smooth continuous  $T(E)$  can be reproduced in any data analysis software simply by re-calculating equation (SE5) using the fitting parameters. A corrected spectrum is then obtained by dividing the raw spectrum by  $T(E)$ .

## **7**      *After Analysis*

When all analyses are complete, please return your results to NPL *via* email or an appropriate file exchange server at the earliest convenience in the format outlined in Section 8. The contents of the VAMAS package do not need to be sent back to NPL.

## **8**      *Data Reporting Format*

Provided with this protocol will be a MS Excel electronic reporting form which will have step-by-step instructions on how to use it. Please report your details, instrument geometry, data and acquisition parameters into this form. We ask that a new form is used for each transmission function you wish to calculate, i.e. for each data set. If you are sending back multiple data reporting forms, then please place them into a .zip folder and name them appropriately.

In the data reporting form, pages 2A and 2B are open sheets with no cell formatting. These spaces should be used to import the kinetic energy and intensity data from the five LDPE datasets and the gold dataset outlined in Section 6.1. For clarity, an example reporting form with model data already included will also be distributed.

Along with the reporting form, please return your raw data files in .vms format and note the filename of the dataset used in each reporting form. Please do not send instrument specific raw data files.

If you wish to send the data in an alternative format, please contact [benjamin.reed@npl.co.uk](mailto:benjamin.reed@npl.co.uk). The preferred method of returning data and reporting forms is by e-mail.

## **9**      *Confidentiality*

The samples supplied in this VAMAS study are not certified reference materials. They are sent to you in confidence and if there are any issues with them upon arrival, we ask that you contact us. Please do not publish or present your results or any details of the analysis used in this study without consulting NPL first. If your laboratory does not want to be identified in our final report, please note this in your data reporting form and inform us by e-mail.

## *Acknowledgements*

The project is supported by the Metrology for Advanced Coatings and Formulated Products theme of the National Measurement System of the UK Department of Business, Energy and Industrial Strategy (BEIS).

## *References*

A. G. Shard and S. J. Spencer. "Intensity calibration for monochromated Al K $\alpha$  XPS instruments using polyethylene", *Surface and Interface Analysis* (2019), Online Version (<https://doi.org/10.1002/sia.6627>)

M. P. Seah and G. Smith. "Quantitative AES and XPS: Determination of the electron spectrometer transmission function and the detector sensitivity energy dependencies for the production of true electron emission spectra in AES and XPS", *Surface and Interface Analysis* (1990), **15**(12), 751-766.

P. J. Cumpson, S. Spencer, and M. Seah. "The Calibration of Auger and X-ray Photoelectron Spectrometers for Valid Analytical Measurements", *Spectroscopy Europe* (1998), **10**, 8-15.



## **S2: VAMAS Project A27 — Participants' Results**

In this section of the supporting information, the key results of VAMAS interlaboratory A27 are presented. **Table S2** shows the important experimental information and values of  $\Delta(\%)$  (the percentage average offset value described by equation 2 in the main article) and  $\Sigma(\%)$  (the percentage systematic deviation value described by Equation 3 in the main article). **Table S2** also contains comments which describe issues or observations with the submitted datasets, or feedback from the participants.

Figures **AA** through to **BI** show the transmission functions derived from both LDPE (green) and gold (orange), for all the participant datasets listed in **Table S2**. In each figure, the values of  $Q_{PE}$  and  $Q_{Au}$  (dots) to which the transmission functions  $T_{PE}$  and  $T_{Au}$  (thick solid lines) are fitted to respectively, are shown. The participant's dataset code is shown in red.

**Table S2. Experimental details and results of VAMAS Project A27**

<b>Code</b>	<b>Spectrometer</b>	<b>Experiment Parameters</b>	<b>Pass Energy (eV)</b>	<b><math>\Delta(\%)</math> 1 d.p.</b>	<b><math>\Sigma(\%)</math> 1 d.p.</b>	<b>Comments</b>
<b>AA</b>	Thermo Scientific / Alpha 110	MonoXPS	100	8.5	2.5	Drop-off in $Q_{Au}$ for kinetic energy around the <i>C KLL</i>
<b>AB-1</b>	Kratos Analytical / Nova	FoV2	160	-5.8	1.5	Sharp increase in $Q_{PE}$ at very low KE not accounted by TPE
<b>AB-2</b>	Kratos Analytical / Nova	FoV1	160	-13.1	2.1	Potential O 1s contamination observed in $Q_{PE}$ .
<b>AC</b>	PHI / VersaProbe II	—	117.4	-14.3	7.0	Variable dark noise causing high kinetic energy deviation
<b>AD-1</b>	Thermo Scientific / Theta 300	PARXPS: FULL angular range	200	29	18.6	Fitting assumes fixed ' <i>a</i> ' angle of 76°; Collection over 22.5 - 77.5° from surface normal; Lots of contamination on LDPE

<b>AD-2</b>	Thermo Scientific / Theta 300	PARXPS: REDUCED angular range	200	39.4	25.2	Fitting assumes fixed ' <i>a</i> ' angle of 76°; Collection over 42.5 - 57.5° from surface normal; Lots of contamination on LDPE
<b>AE-1</b>	PHI / VersaProbe II	Normal	187.9	2.6	2.7	Intensity mismatch observed in $Q_{PE}$ across the C 1s region.
<b>AE-2</b>	PHI / VersaProbe II	Normal	93.9	-5.3	2.7	—
<b>AE-3</b>	PHI / VersaProbe II	Normal	46.5	-5.8	7.5	Increased deviation between $T_{PE}$ and $T_{Au}$ at HKE.
<b>AE-4</b>	PHI / VersaProbe II	Normal	29.4	-7.4	5.0	—
<b>AF</b>	Kratos Analytical / Axis Ultra DLD	Hybrid; Slot	160	-11.7	4.3	Gold signal is saturating detector
<b>AG</b>	Thermo Scientific / Nexsa	Standard	150	-0.7	3.6	Gold signal is saturating detector; O 1s visible in LDPE; evidence of internal scattering around carbon peaks
<b>AH</b>	PHI / VersaProbe II	Normal	187	3.0	10.3	Potentially different X-ray power used (correction factor used of 2.22 used on LDPE)
<b>AI</b>	Scienta Omicron / UHV System	High Magnification	160	16.6	6.9	$T_{PE}$ higher than $T_{Au}$
<b>AJ-1</b>	ULVAC-PHI / Quantum 2000	400sw	188	-9.6	3.6	No dark noise correction, caused step at C 1s
<b>AJ-2</b>	ULVAC-PHI / Quantum 2000	100sw	188	-8.3	5.8	No dark noise correction, caused step at C 1s
<b>AK-1</b>	SPECS / PHOIBOS 150	FAT; Medium Area	60	-4.2	15.4	Significant deviation of transmission functions at high kinetic energy

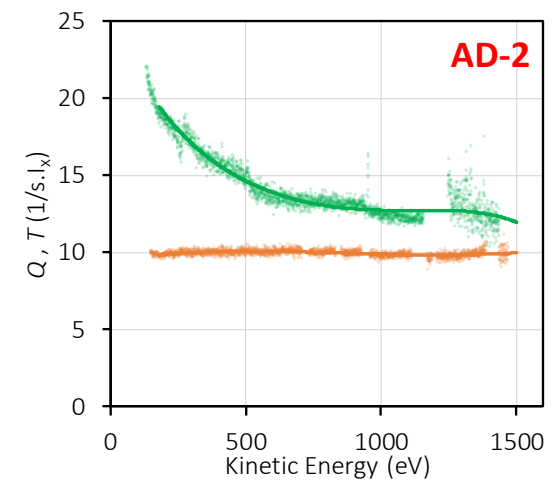
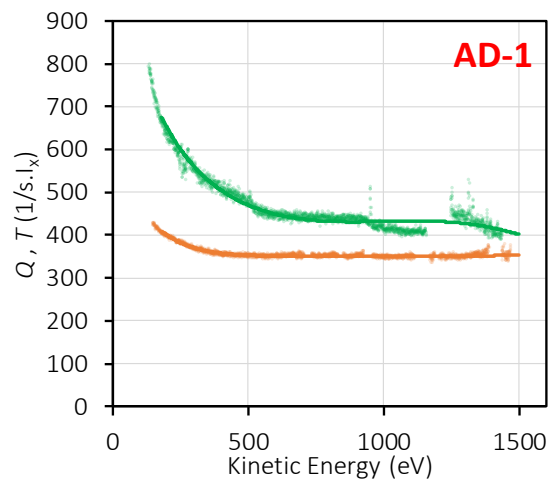
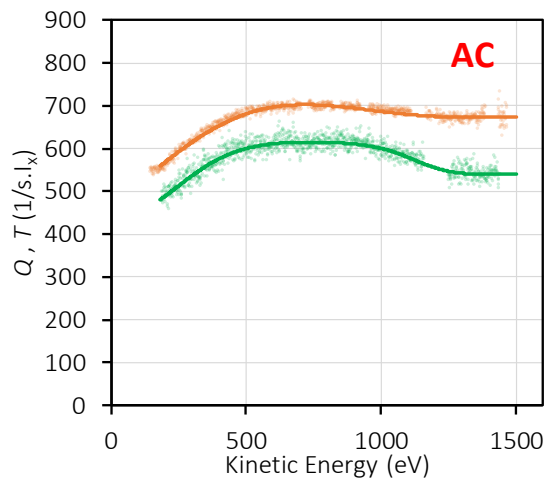
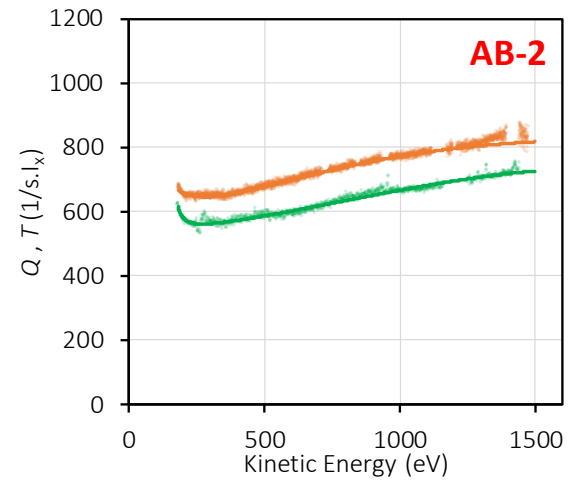
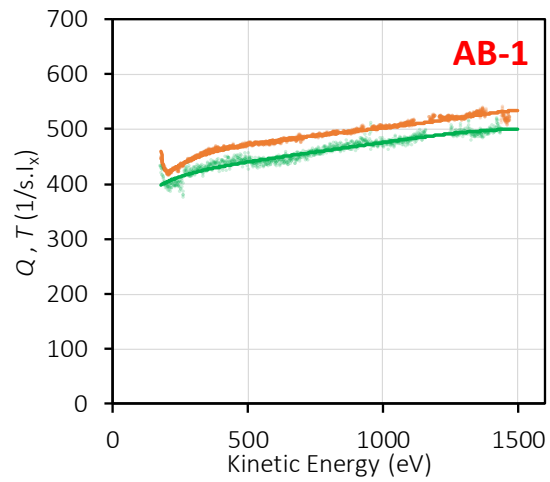
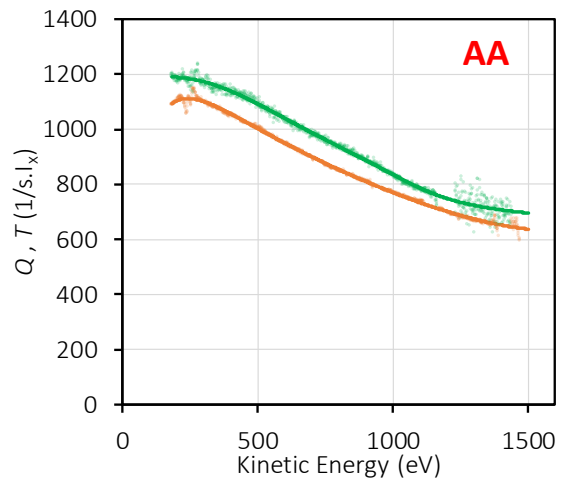
<b>AK-2</b>	SPECS / PHOIBOS 150	FAT; Medium Area	30	5.3	17.0	Very different transmission function shapes
<b>AL</b>	PHI / VersaProbe II	—	117.5	-1.6	3.8	Very low signal-to-noise in $Q_{PE}$ , but despite that, very good agreement between $T_{PE}$ and $T_{Au}$ .
<b>AM-1</b>	Kratos Analytical / Axis 165	Hybrid; Slit 0.5; Aperture 0.5	160	-8.0	7.0	Low kinetic energy region corrected by a factor of ~1.6. Possible error in geometry: better fit using $a = 60^\circ$
<b>AM-2</b>	Kratos Analytical / Axis 165	Hybrid; Slit 0.5; Aperture 0.5	40	8.5	5.2	Possible error in geometry: better fit using $a = 60^\circ$ .
<b>AN-0</b>	SPECS / PHOIBOS 100	FAT; Medium Area	30	7.6	42.4	Old dataset with different spectrometer, replaced with new data but shown in Figure 3 in main manuscript for demonstration of large $\Sigma(\%)$ .
<b>AN-1</b>	SPECS / PHOIBOS 150	FAT; Medium Area	100	0.0	3.2	Contamination peak on LDPE at ~1400 eV, sputtered gold?
<b>AN-2</b>	SPECS / PHOIBOS 150	FAT; Medium Area	50	-0.3	3.0	Contamination peak on LDPE at ~1400 eV, sputtered gold?
<b>AN-3</b>	SPECS / PHOIBOS 150	FAT; Medium Area	25	0.0	3.2	Contamination peak on LDPE at ~1400 eV, sputtered gold?
<b>AO-1</b>	Kratos Analytical / Axis Ultra DLD	Electrostatic; Slot	160	3.1	12.9	Significant deviation between $T_{PE}$ and $T_{Au}$ at low KE (<500 eV), possibly due to tungsten contamination on LDPE; ageing MCP at detector
<b>AO-2</b>	Kratos Analytical / Axis Ultra DLD	Electrostatic; Slot	20	-19.5	13.7	Cubic function used to fit $Q_{PE}$ due to signal-to-noise, ~20 % absolute offset between $T_{PE}$ and $T_{Au}$ across entire KE range; Deviation between $T_{PE}$ and $T_{Au}$ , possibly due to

						tungsten contamination on LDPE ageing MCP at detector
<b>AP-1</b>	Kratos Analytical / Axis Ultra DLD	Hybrid	160	-2.6	8.2	Large deviation between transmission functions at high kinetic energy, possible dark noise issue
<b>AP-2</b>	Kratos Analytical / Axis Ultra DLD	Hybrid	40	-13.0	4.3	$T_{PE}$ significantly lower than $T_{Au}$
<b>AP-3</b>	Kratos Analytical / Axis Ultra DLD	Electrostatic	160	-17.3	8.0	$T_{PE}$ significantly lower than $T_{Au}$
<b>AQ</b>	Thermo Scientific / VG ESCALab 250 Xi	Hybrid	100	-0.2	2.2	Variable dark noise, corrected with an arbitrary function
<b>AR</b>	PHI / VersaProbe III	—	140	-3.1	14.1	Significant carbon and oxygen contamination on Gold.
<b>AS-1</b>	Kratos Analytical / Axis Ultra DLD	Hybrid; Slot	160	-18.6	6.1	$T_{Au}$ is ~20 % higher than $T_{PE}$ ; F:I ratio deviates from unity by 10 % at low kinetic energy, variable dark noise?
<b>AS-2</b>	Kratos Analytical / Axis Ultra DLD	FoV1; Slot	160	96.9	10.8	$T_{PE}$ is ~100 % higher than $T_{Au}$ ; F:I ratio deviates from unity by 10 % at low kinetic energy, variable dark noise; Fitting failed to account for transmission function variability
<b>AS-3</b>	Kratos Analytical / Axis Ultra DLD	FoV1; Slot	80	-11.6	11.2	$T_{Au}$ is ~10 % higher than $T_{PE}$ ; F:I ratio deviates from unity by 10 % at low kinetic energy to 20 % at high kinetic energy, variable dark noise; Fitting failed to account for transmission function variability
<b>AT</b>	SPECS / PHOIBOS 150	Medium Area	50	3.8	4.7	Sloped F:I ratio

<b>AU-1</b>	PHI / Quantera II Hybrid	FAT	224	-2.8	7.9	Variable dark noise, corrected with an arbitrary function $f(E)$
<b>AU-2</b>	PHI / Quantera II Hybrid	FAT	112	-2.6	4.0	Variable dark noise, corrected with an arbitrary function $f(E)$
<b>AV</b>	Surf Sci / SSX-100	—	—	-13.3	9.6	Significant carbon and oxygen contamination on Gold; $T_{Au}$ fitting excludes data below 400 eV kinetic energy
<b>AW-1</b>	Kratos Analytical / Axis Supra	Hybrid; Large Area	160	5.2	4.4	$T_{PE}$ is ~500 % higher than $T_{Au}$ ; X-ray power scaling difference (correction factor of 0.2 used on $I_{PE}$ ), possible detector saturation observed in $Q_{Au}$
<b>AW-2</b>	Kratos Analytical / Axis Supra	Hybrid; Large Area	40	2.2	21.2	Significant error between $T_{PE}$ and $T_{Au}$ , possible detector saturation observed in $Q_{Au}$
<b>AX</b>	SPECS / PHOIBOS 150	Medium Area	50	-4.3	1.5	Variable dark noise, corrected with an arbitrary function
<b>AY</b>	ULVAC-PHI / Quantera SXM	Standard	280	-4.6	4.3	Variable dark noise
<b>AZ-1</b>	Thermo Scientific / Nexsa	CAE, Standard	200	-1.1	5.0	Gold signal is saturating detector, non-linearity, scattering around C 1s
<b>AZ-2</b>	Thermo Scientific / Nexsa	CAE, Standard	200	28.1	5.8	Gold signal is saturating detector, non-linearity, $T_{PE}$ is ~20 % higher than $T_{Au}$ , scattering around C 1s
<b>AZ-3</b>	Thermo Scientific / ESCALAB	CAE, Standard	200	70.0	8.9	Gold signal is saturating detector, non-linearity, $T_{PE}$ is ~70 % higher than $T_{Au}$
<b>BA</b>	Kratos Analytical / Axis Supra	Hybrid; Slot	160	-0.5	4.6	Gold signal is saturating detector, non-linearity around C 1s region

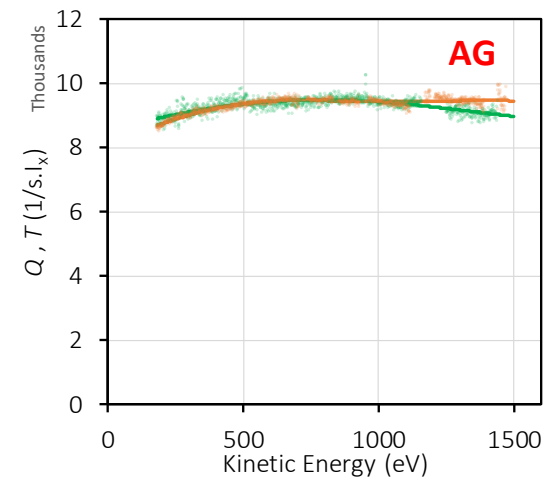
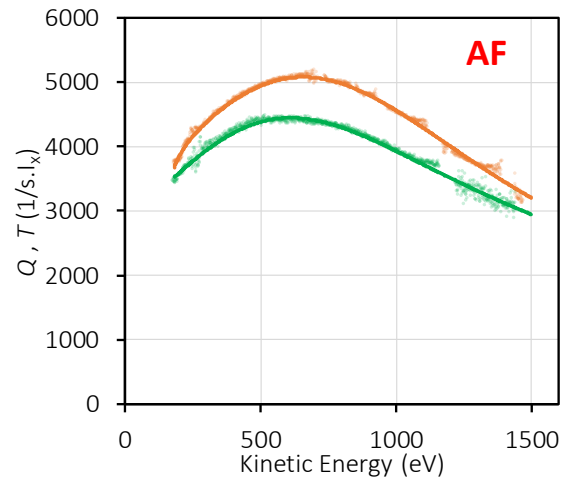
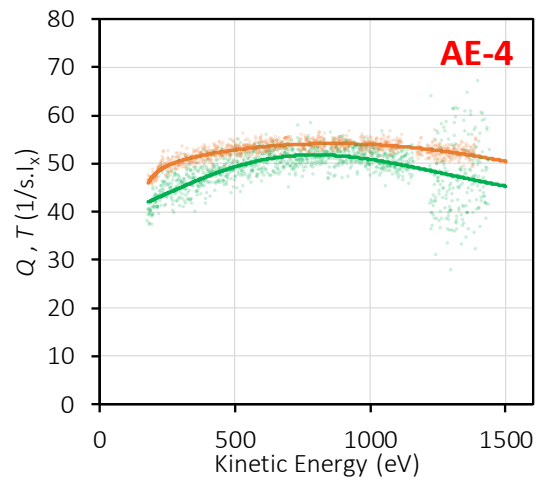
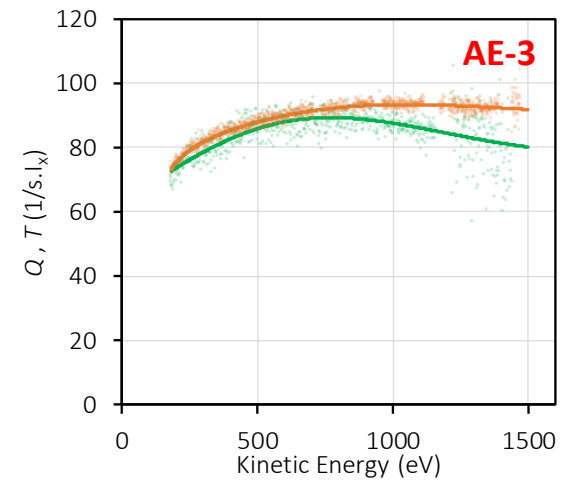
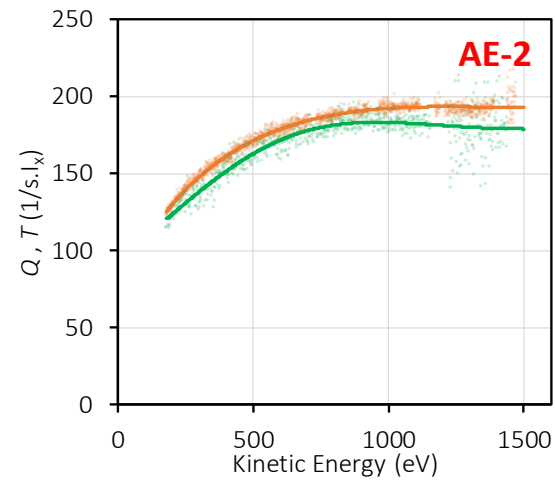
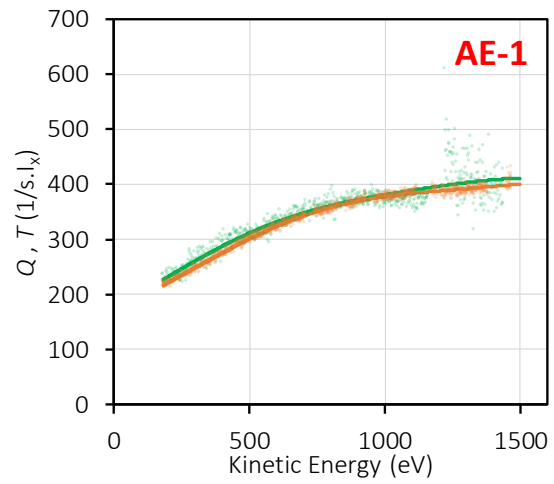
<b>BB</b>	PHI / Quantera Hybrid	Scanned Mode	224	65.5	3.9	$T_{PE}$ is ~65 % higher than $T_{Au}$ , insufficient X-ray warm-up
<b>BC</b>	ULVAC-PHI / Quantera SXM	—	280	-2.8	2.8	F:I Ratio ~0.95 but otherwise flat
<b>BD</b>	SSI / S-Probe	Standard Retardation Mode	150	—	—	Fitting of LDPE failed, unknown issues, catastrophic loss of counts at low kinetic energy
<b>BE-1</b>	Kratos Analytical / Axis Ultra DLD	Hybrid; Slot	160	-1.2	2.3	Sloped F:I ratio
<b>BE-2</b>	Kratos Analytical / Axis Ultra DLD	Hybrid; Slot	40	-5.6	5.9	Increased deviation between $T_{PE}$ and $T_{Au}$ at HKE.
<b>BF-1</b>	Thermo Scientific / ESCALAB Xi+	Standard; Slit 900	160	-1.3	2.2	Small deviation around the C <i>KLL</i> peak
<b>BF-2</b>	Thermo Scientific / ESCALAB Xi+	Standard; Slit 900	100	-7.7	2.2	Small deviation around the C <i>KLL</i> peak
<b>BF-3</b>	Thermo Scientific / ESCALAB Xi+	Standard; Slit 500	160	0.4	1.7	Small deviation around the C <i>KLL</i> peak
<b>BF-4</b>	Thermo Scientific / ESCALAB Xi+	Standard; Slit 500	100	-0.9	1.7	Small deviation around the C <i>KLL</i> peak
<b>BF-5</b>	Thermo Scientific / ESCALAB Xi+	Electro; Slit 900	160	8.0	4.1	$T_{PE}$ is higher than $T_{Au}$ , insufficient X-ray warm-up or Electrostatic mode issue?
<b>BF-6</b>	Thermo Scientific / ESCALAB Xi+	Electro; Slit 900	100	9.9	4.2	$T_{PE}$ is higher than $T_{Au}$ , insufficient X-ray warm-up or Electrostatic mode issue?
<b>BF-7</b>	Thermo Scientific / ESCALAB Xi+	Electro; Slit 500	160	-2.8	1.4	—

<b>BF-8</b>	Thermo Scientific / ESCALAB Xi+	Electro; Slit 500	100	11.5	6.6	$T_{PE}$ is higher than $T_{Au}$ , insufficient X-ray warm-up or Electrostatic mode issue?
<b>BG-1</b>	Thermo Scientific / VG ESCALAB 220i-XL	Large Area	160	6.5	4.3	Possible variable dark noise
<b>BG-2</b>	ULVAC-PHI / ESCA 5800	Omni V Minimum area	187.9	5.4	3.5	Possible variable dark noise
<b>BH</b>	Kratos Analytical / Axis Ultra DLD	Hybrid; Slot	80	-13.4	12.4	Different X-ray power used (LDPE @ 150 W, Au @ 45 W), correction factor used (0.3)
<b>BI</b>	Kratos Analytical / Axis Ultra DLD	Hybrid; Slot	80	—	—	Lots of contamination on LDPE; No gold spectrum submitted.

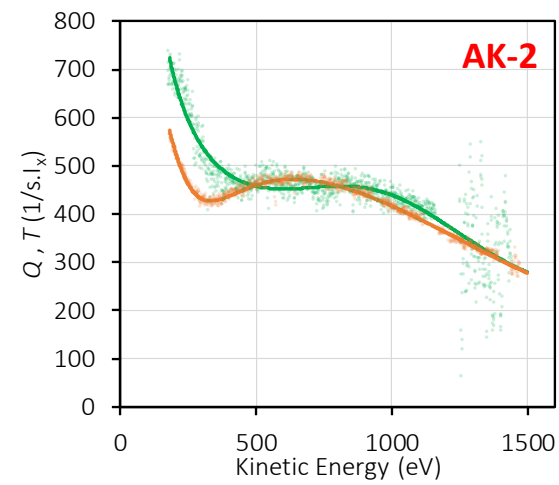
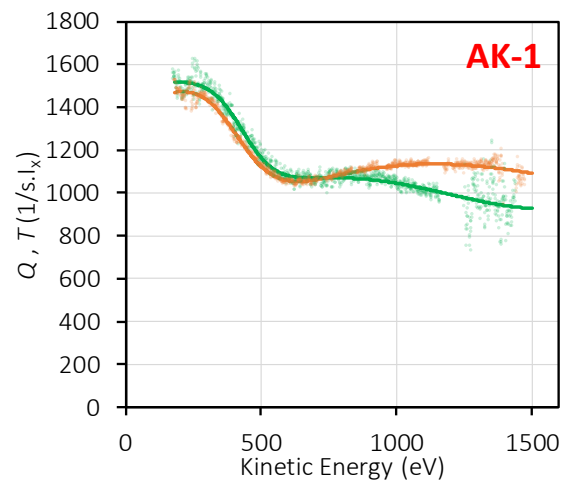
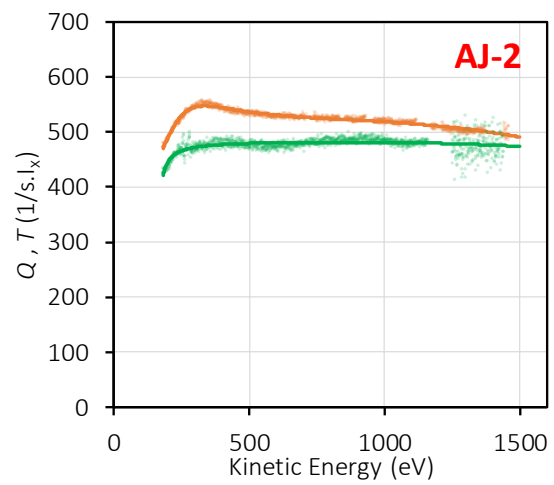
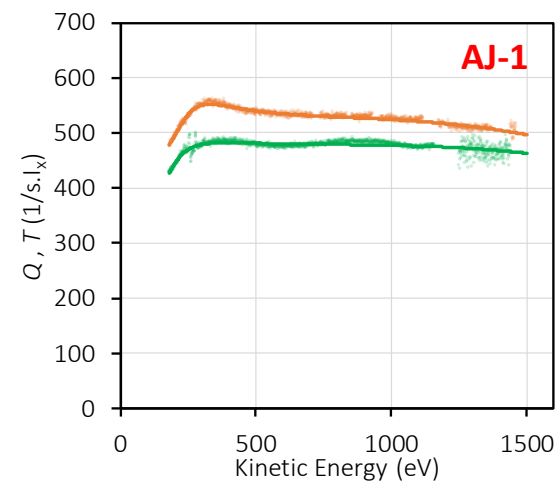
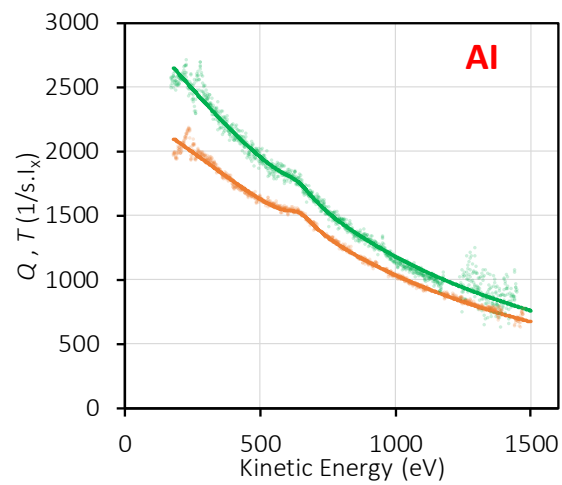
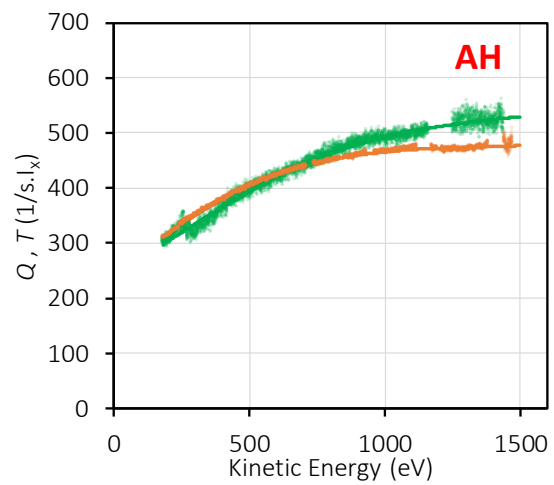


	Q	T
PE	<span style="color: green;">●</span>	<span style="color: green;">—</span>
Au	<span style="color: orange;">●</span>	<span style="color: orange;">—</span>

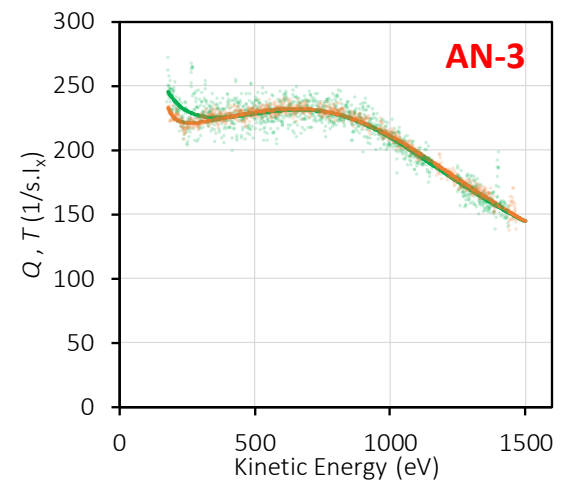
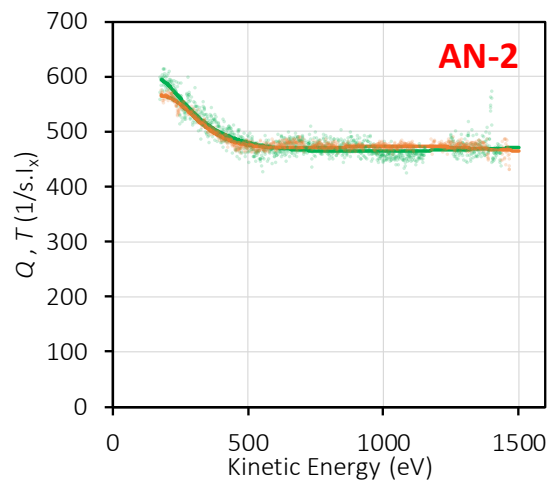
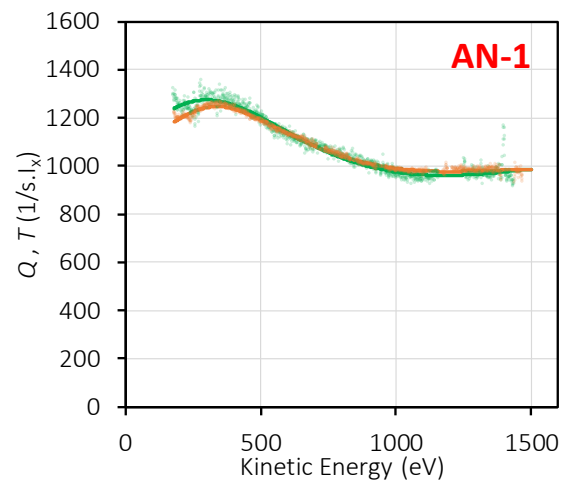
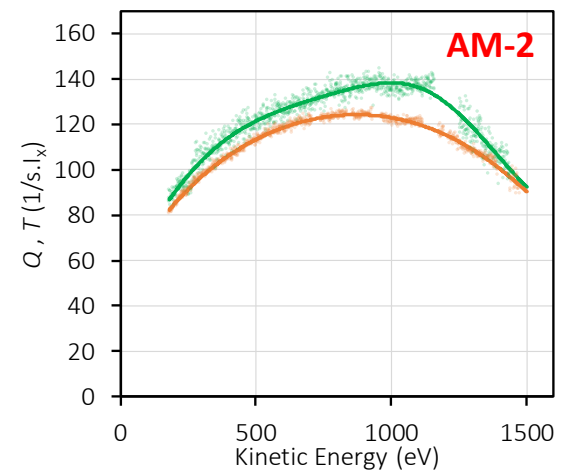
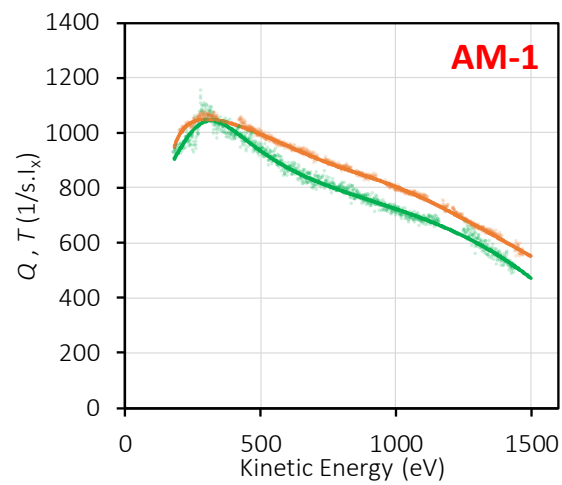
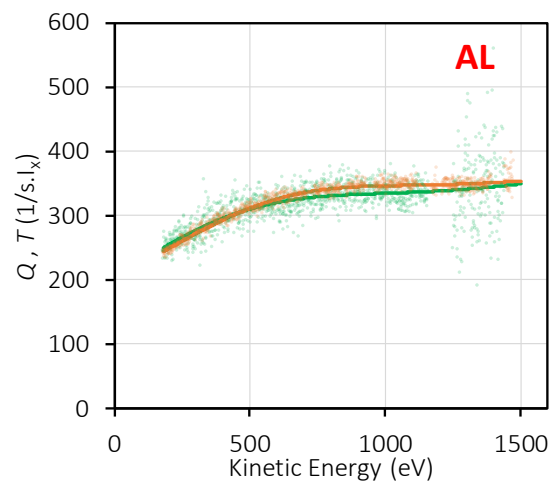




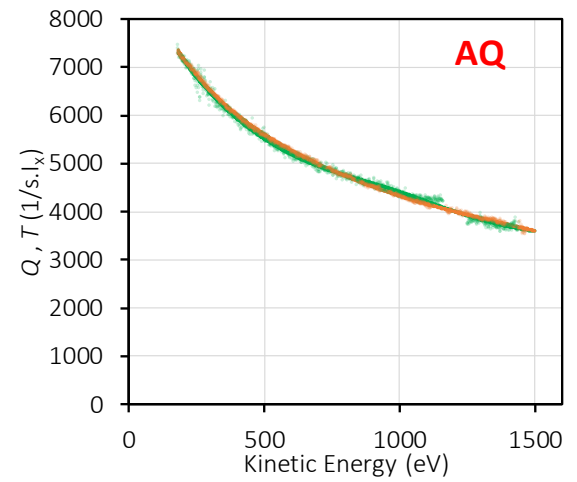
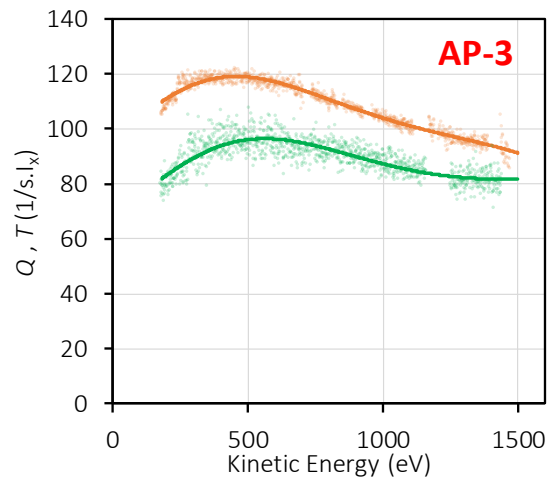
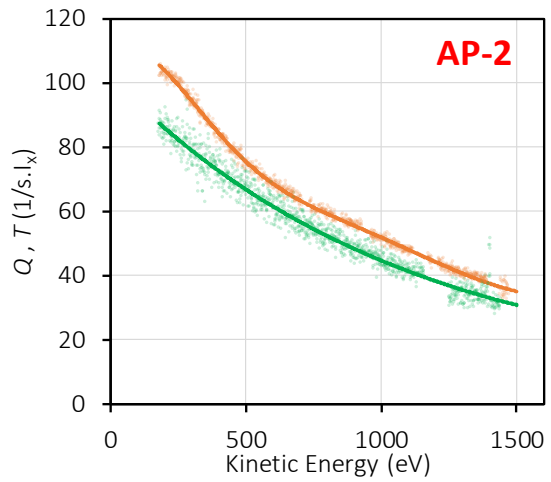
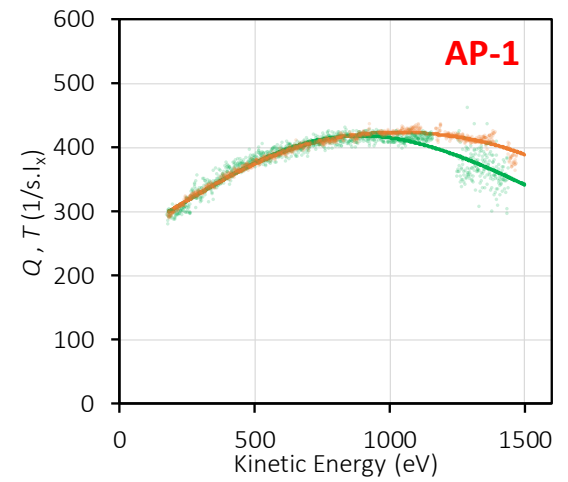
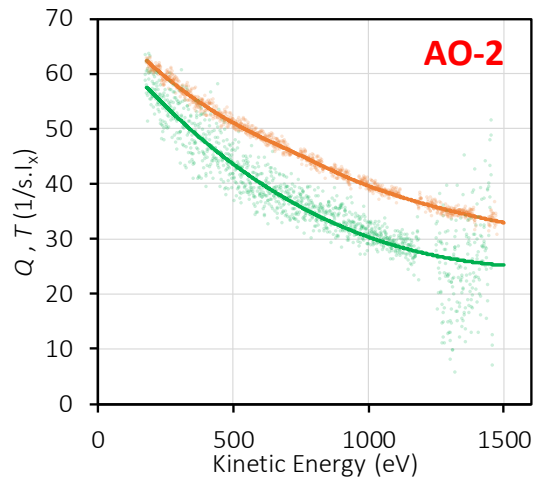
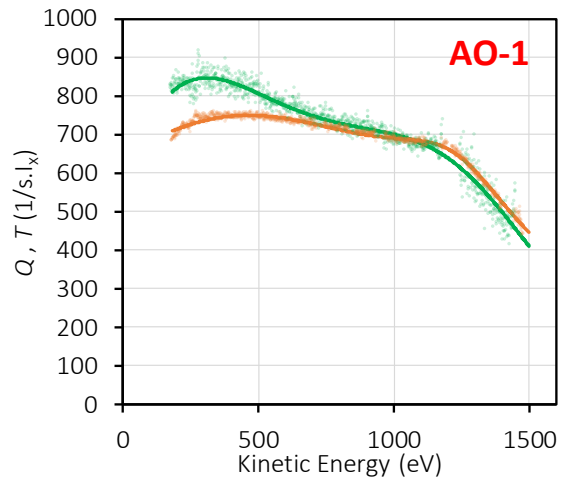
	Q	T
PE	<span style="color: green;">●</span>	<span style="color: green;">—</span>
Au	<span style="color: orange;">●</span>	<span style="color: orange;">—</span>



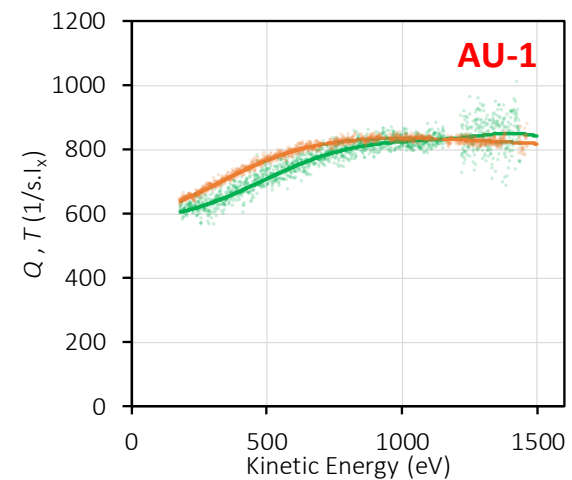
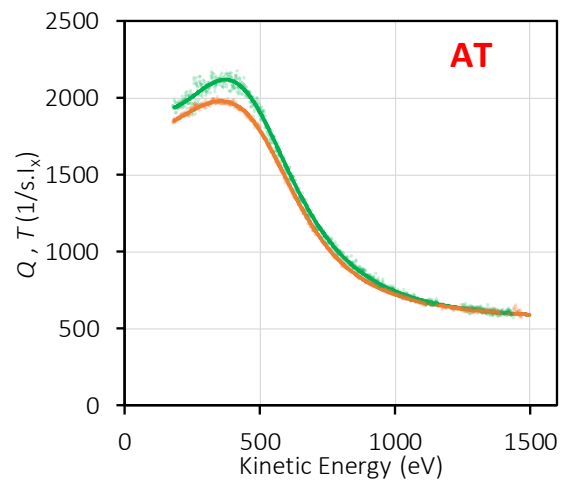
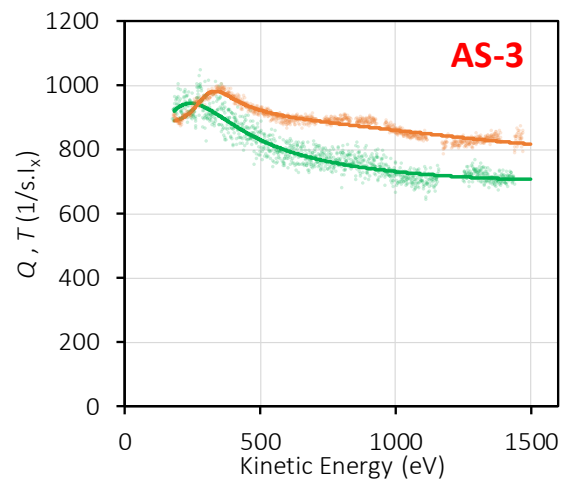
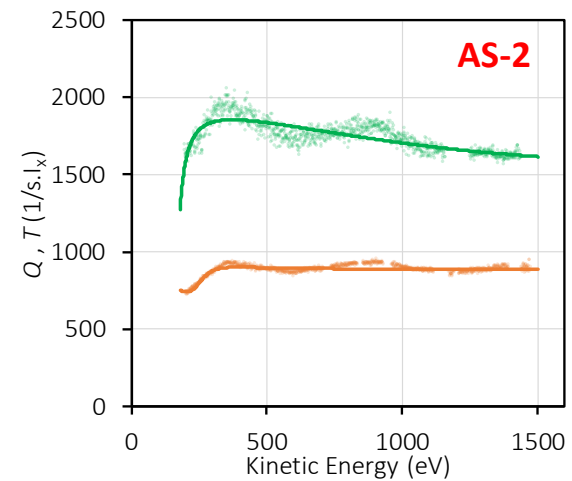
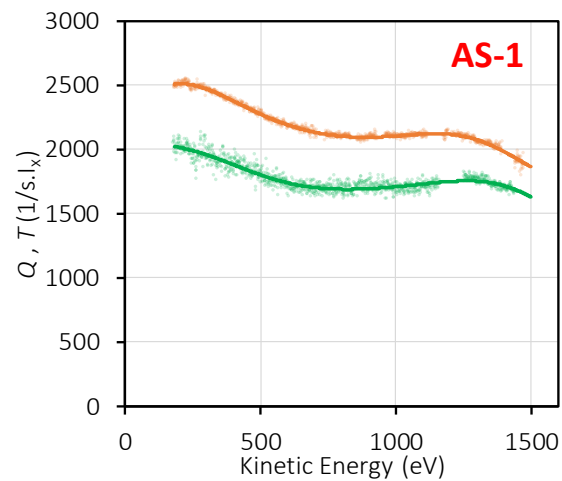
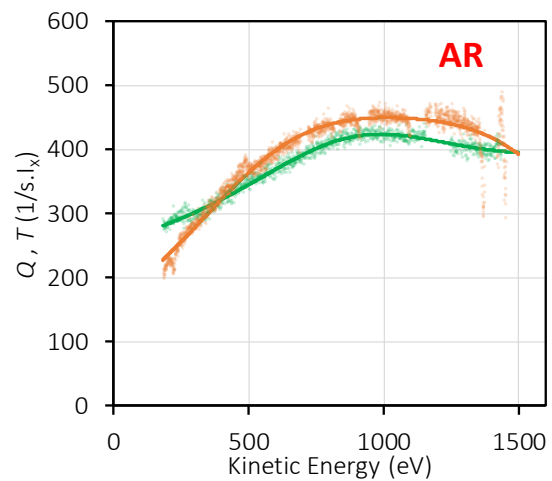
	Q	T
PE	<span style="color: green;">●</span>	<span style="color: green;">—</span>
Au	<span style="color: orange;">●</span>	<span style="color: orange;">—</span>



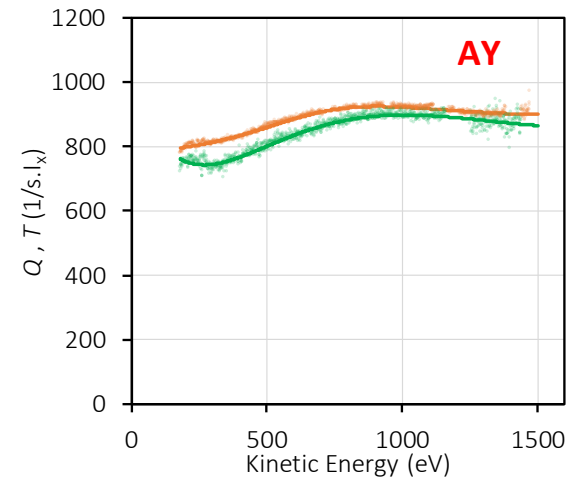
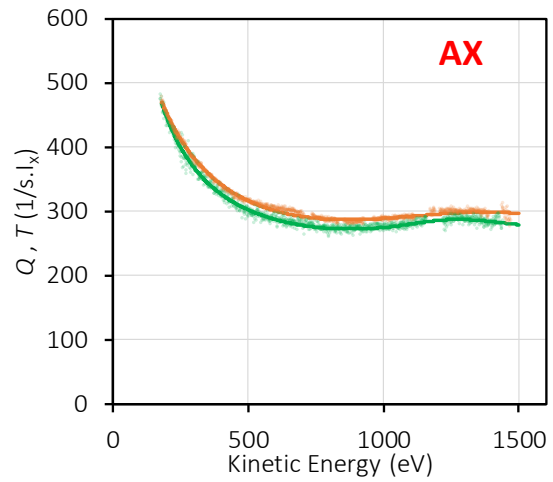
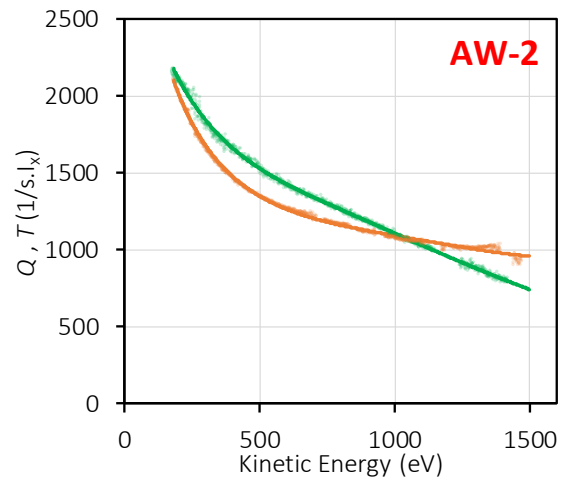
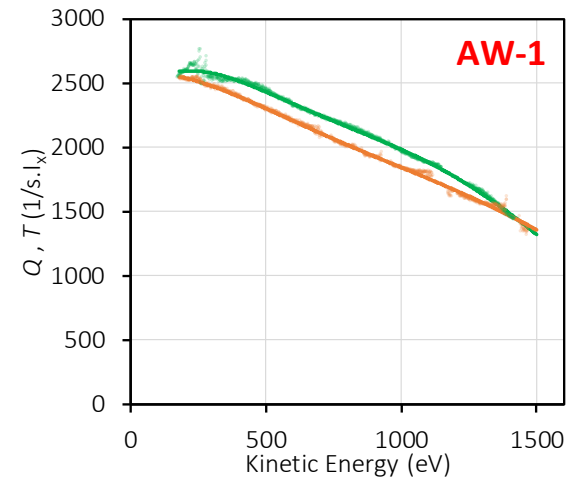
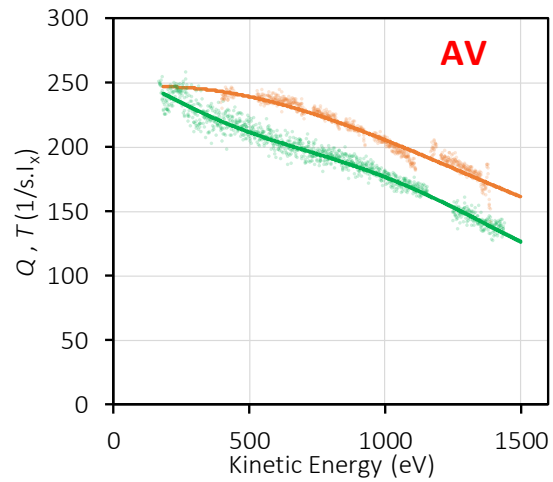
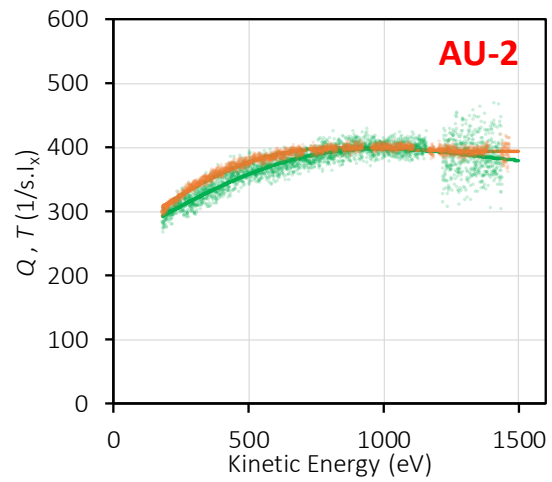
	Q	T
PE	<span style="color: green;">●</span>	<span style="color: green;">—</span>
Au	<span style="color: orange;">●</span>	<span style="color: orange;">—</span>



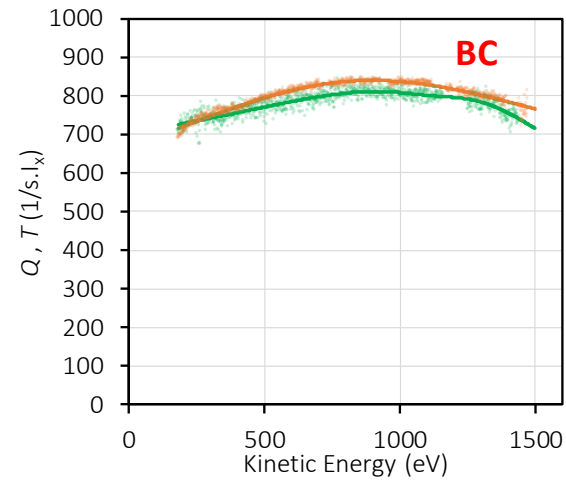
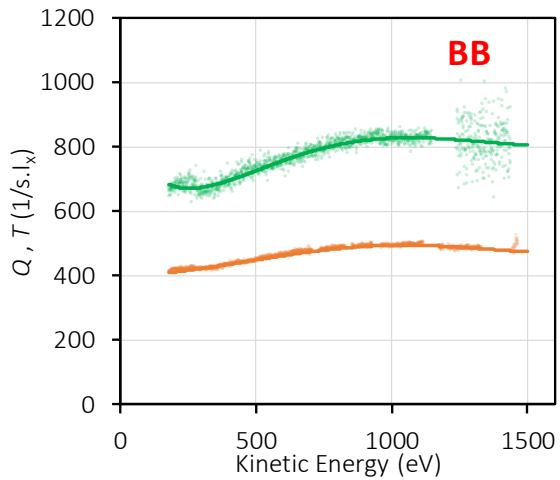
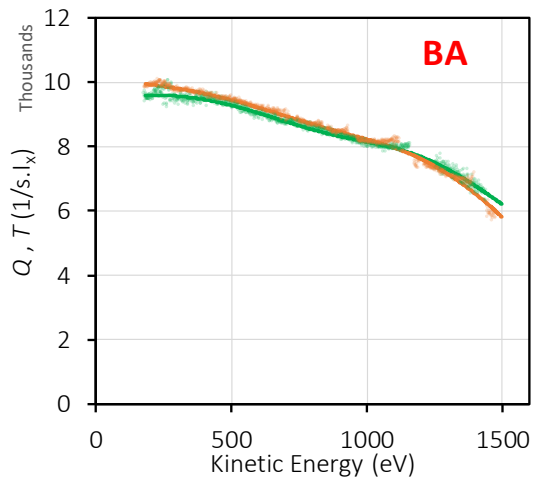
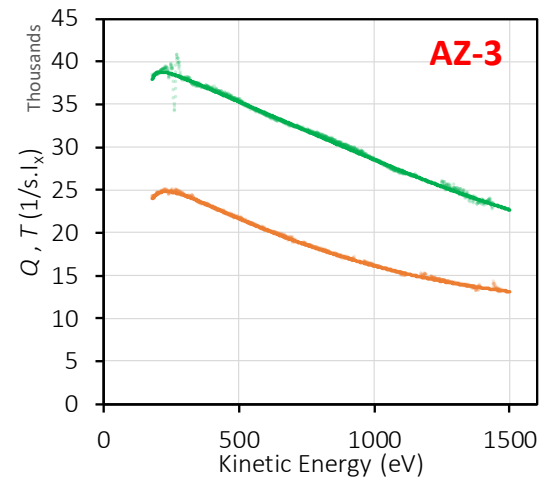
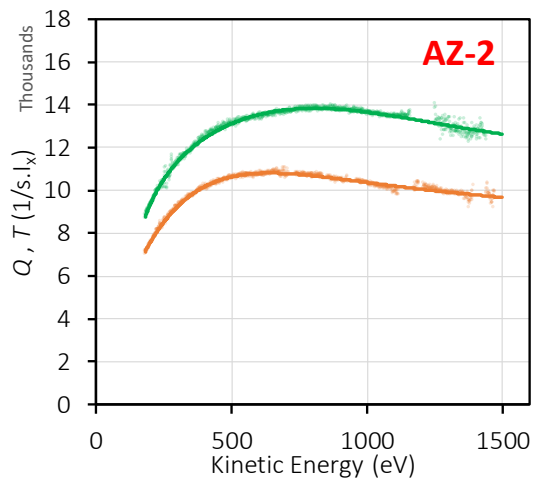
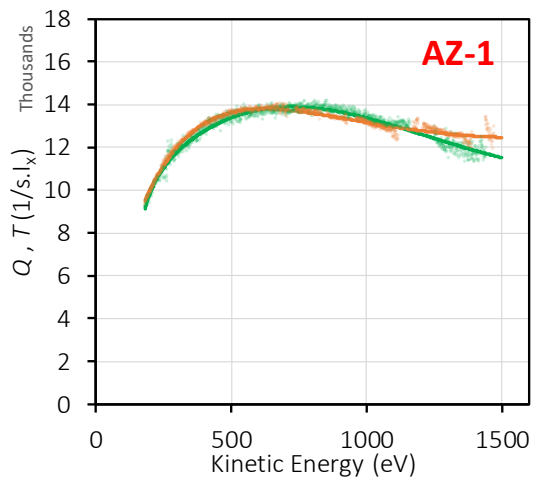
	Q	T
PE	<span style="color: green;">●</span>	<span style="color: green;">—</span>
Au	<span style="color: orange;">●</span>	<span style="color: orange;">—</span>



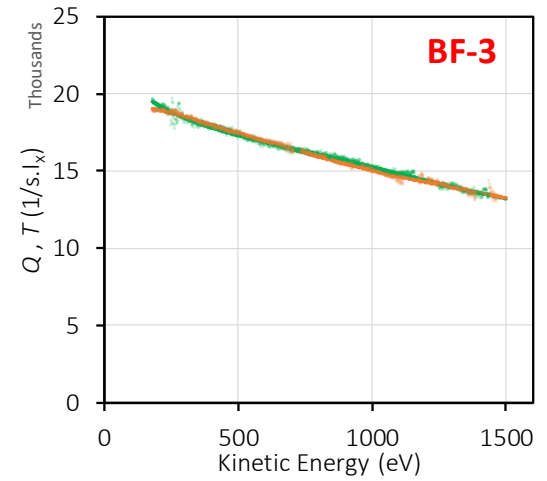
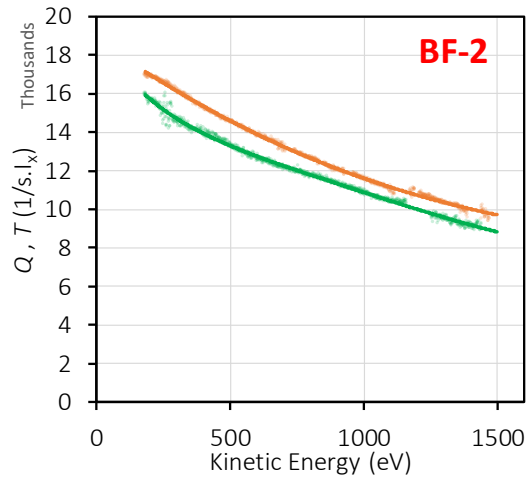
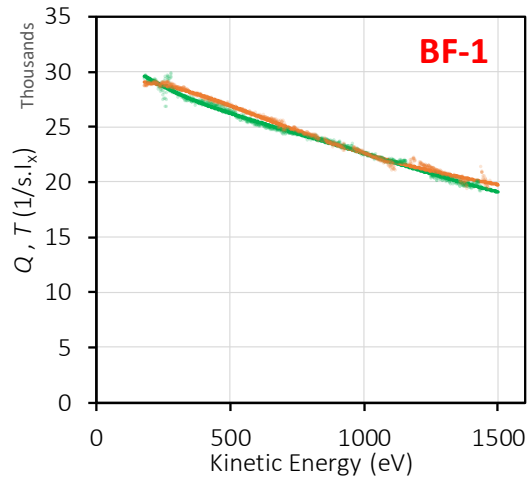
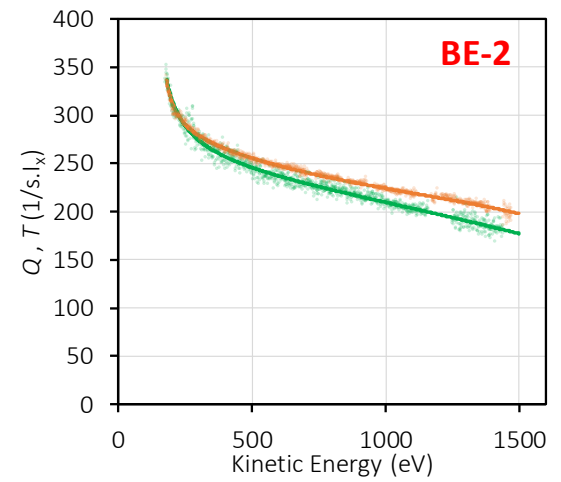
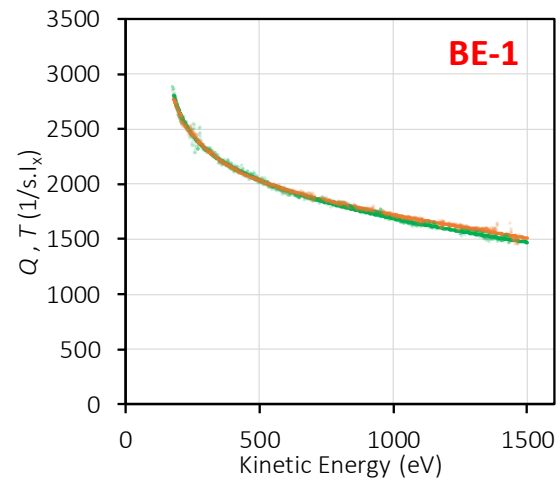
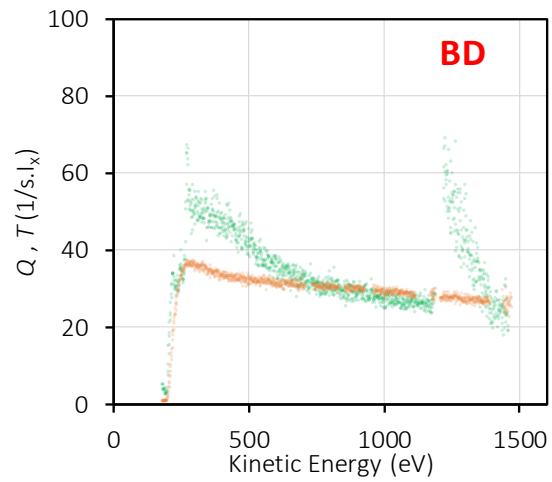
	Q	T
PE	<span style="color: green;">●</span>	<span style="color: green;">—</span>
Au	<span style="color: orange;">●</span>	<span style="color: orange;">—</span>



	Q	T
PE	<span style="color: green;">●</span>	<span style="color: green;">—</span>
Au	<span style="color: orange;">●</span>	<span style="color: orange;">—</span>

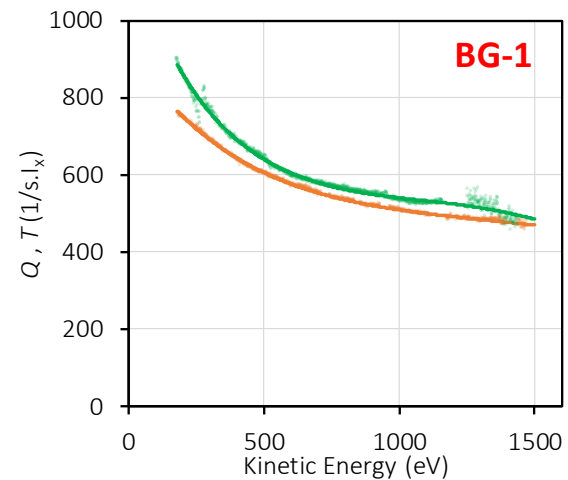
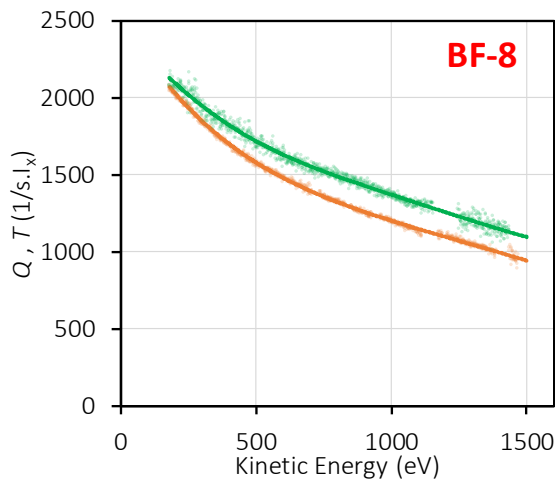
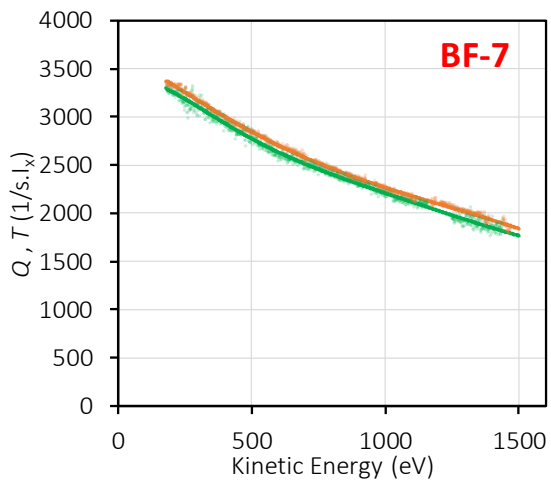
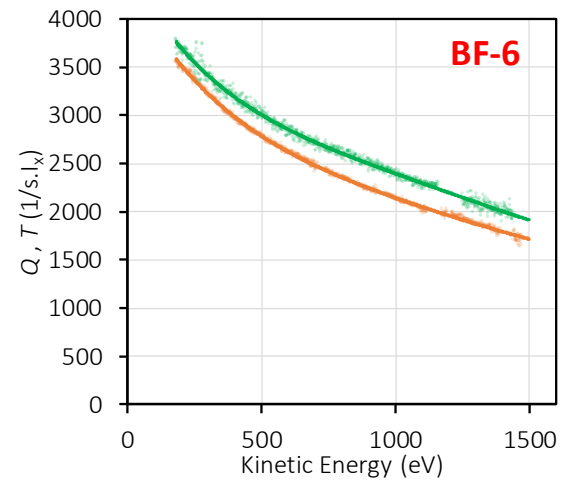
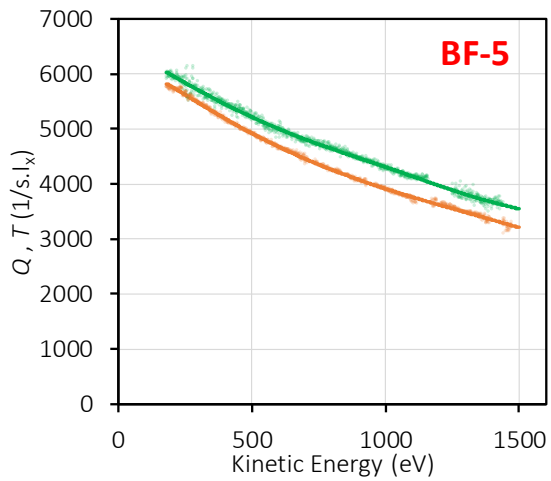
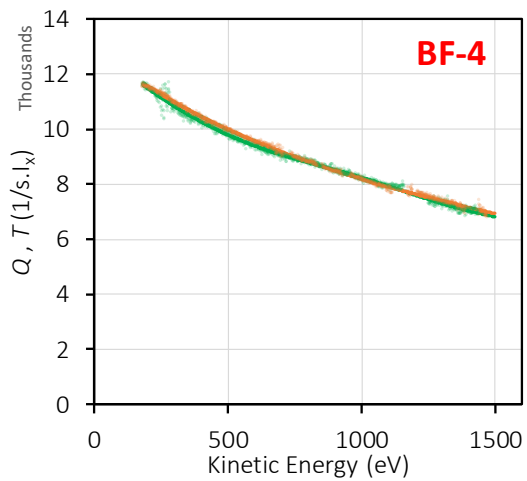


	Q	T
PE	<span style="color: green;">●</span>	<span style="color: green;">—</span>
Au	<span style="color: orange;">●</span>	<span style="color: orange;">—</span>

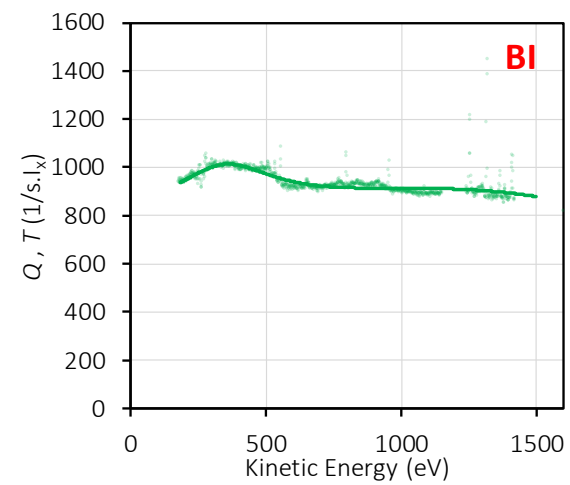
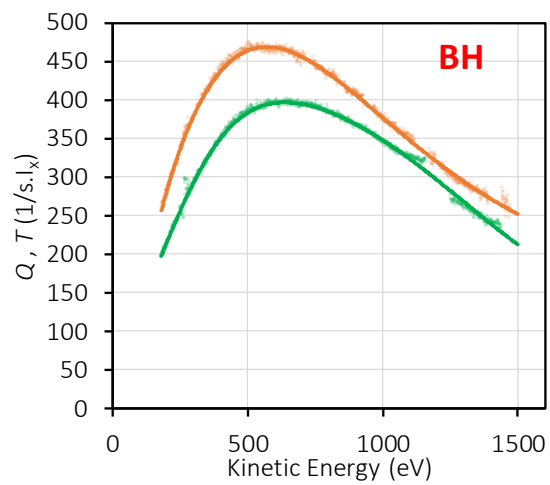
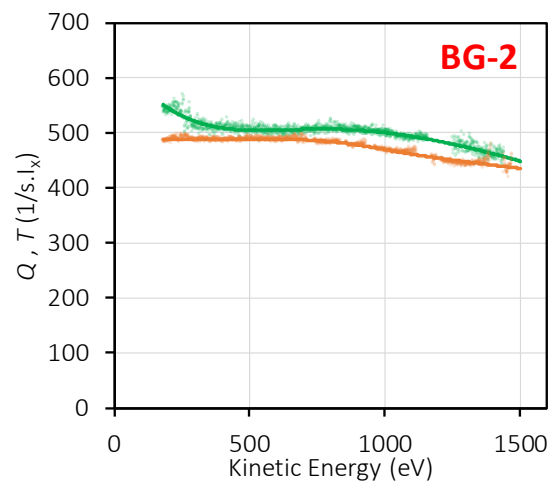


	Q	T
PE	<span style="color: green;">●</span>	<span style="color: green;">—</span>
Au	<span style="color: orange;">●</span>	<span style="color: orange;">—</span>





	Q	T
PE	<span style="color: green;">●</span>	<span style="color: green;">—</span>
Au	<span style="color: orange;">●</span>	<span style="color: orange;">—</span>



	$Q$	$T$
PE		
Au		

### S3: Additional Figures

$$\Delta = \left[ \left( \frac{1}{n} \sum_{i=1}^n R_i \right) - 1 \right] = [\bar{R} - 1] \quad \Sigma = \frac{2\sigma_R}{\bar{R}}$$

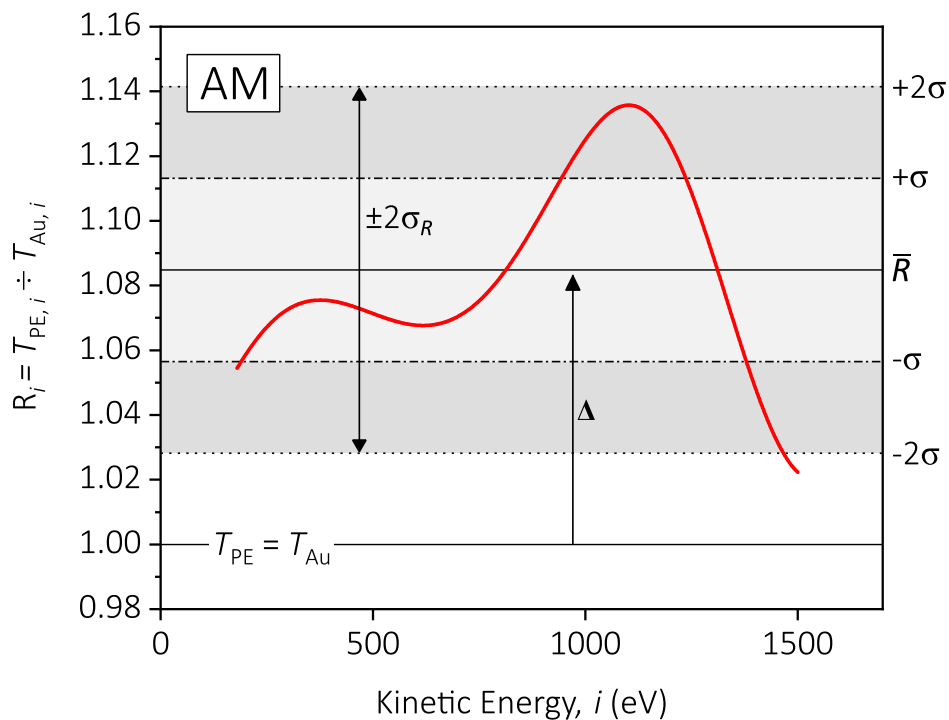


**Figure S7.** The values of  $R_i$  extracted from participant AM's data. The red curve shows the ratio  $R$  between  $T_{PE}$  and  $T_{Au}$  with kinetic energy  $i$ . The mean value of  $R_i$ , denoted by  $\bar{R}$ , is shown by the solid line at  $\sim 1.085$ . The dot-dash lines show the values of  $R_i$  that are one standard deviation,  $\sigma$ , away from  $\bar{R}$ ; the corresponding light grey region contains the values of  $R_i$  that are within  $\bar{R} \pm \sigma$ . Similarly, the dotted lines show the values of  $R_i$  that are two standard deviations,  $2\sigma$ , away from  $\bar{R}$ ; the corresponding dark grey region (including the light grey region) contains the values of  $R_i$  that are within  $\bar{R} \pm 2\sigma$ . The solid line at  $R_i = 1.00$  (unity) shows the case where  $T_{PE} = T_{Au}$  for any kinetic energy  $i$ . Given that this is the optimal case, the difference between unity and  $\bar{R}$  is given by  $\Delta$ , and represents the offset factor between  $T_{PE}$  and  $T_{Au}$ .

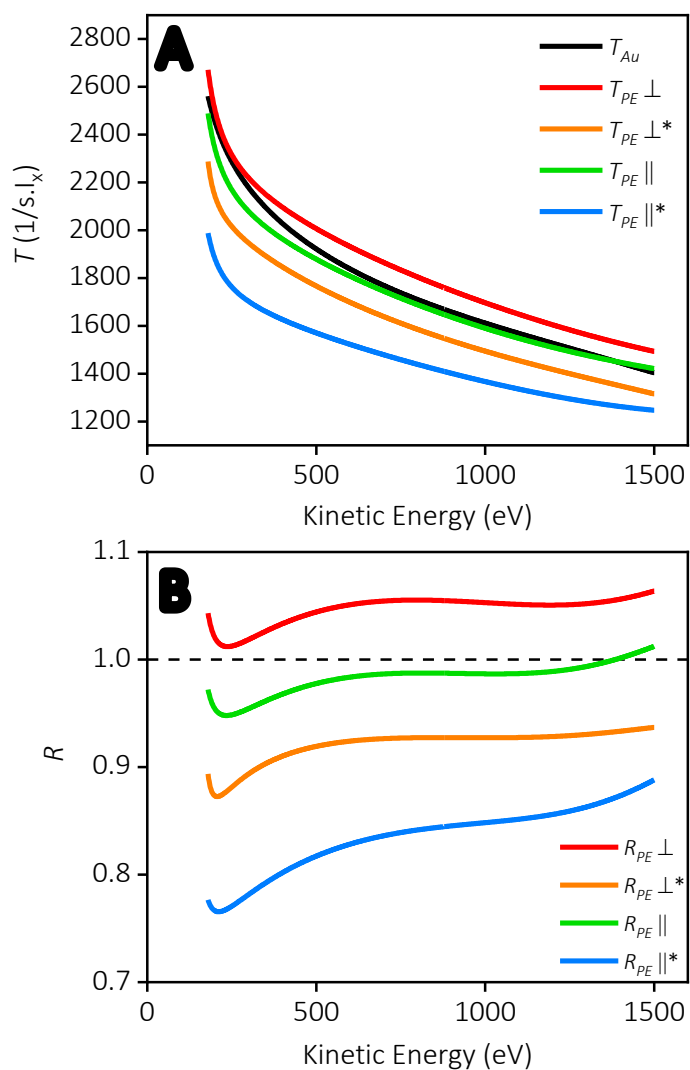


**Figure S8.** (A)  $T_{PE}$  and  $T_{Au}$  calculated from LDPE spectra acquired by NPL. The LDPE was prepared by scraping the surface using a clean scalpel either parallel ( $\parallel$ ) or perpendicular ( $\perp$ ) to the source-analyser plane. Some samples were over-scraped in order to obtain a visibly rough surface (\*). (B) The ratios  $R$  calculated from panel A. The parallel ( $\parallel$ ) scraped LDPE provided the closest  $R$  to unity.